**TECHNISCHE UNIVERSITÄT DRESDEN**

# Stochastical Dynamics of Open Quantum Systems

Diplomarbeit

zur Erlangung des wissenschaftlichen Grades

Diplom-Physiker

vorgelegt von

Daniel Süß

geboren am 18.10.1987 in Dresden

Institut für Theoretische Physik

der Technischen Universitaet Dresden

2013

1. Gutachter:   Herr Prof. Dr. Walter T. Strunz

# Zusammenfassung

# Abstract

# Contents

# 1. Introduction

The explanation of the discrete Hydrogen-spectrum in terms of Matrix-mechanics by Heisenberg and Wave-mechanics by Schrödinger is often perceived as the hour of birth for modern quantum theory. Since then, the desire to understand systems with an increasing number of degrees of freedom and ever-growing complexity has been a main driving force behind the development of new theoretical ideas. However, the overwhelming majority of quantum mechanical insights relies on more or less severe approximations, as even apparently simple models like the Helium atom have not been solved analytically. One simplification that underlies all physical investigation is the distinction between relevant and irrelevant degrees of freedom for a certain situation: Even the simple Hydrogen model, made up from an electron-proton pair and the mutual Coulomb attraction, ignores the surrounding electrons and protons in the same container, to give an example. While under many circumstances the relevant degrees of freedom behave like an isolated unit, there are examples where environmental effects significantly shape the dynamical behavior of the system under consideration—these are referred to as open quantum systems. Clearly, the cut distinguishing between relevant system and irrelevant environment is not uniquely defined, but generally, the requirement to account for a given experimental setting eliminates ambiguities to the greatest possible extent.

Of course, the previous discussion applies not only to quantum mechanics: A closed classical system is described by phase space coordinates $(p, q)$ and canonical equations of motion in the Hamiltonian framework. To account for the influence of an environment, the latter are simply extended by fluctuation- and friction-forces leading to an irreversible time evolution governed by the stochastic Langevin equation [20]. A different description arises by averaging trajectories corresponding to different noise-realizations, the resulting probability density on phase space satisfies the Fokker-Planck equation. However, both points of view are completely equivalent; there is no conceptual problem in assigning a pure state, namely a phase space point $(p(t), q(t))$,

to a given trajectory at any time $t$—this simplifies matters dramatically compared to an open quantum system.

## 1.1. Open Quantum Systems

In order to determine the dynamics of an open quantum system from first principles, we proceed as follows: First we embed the system into an environment such that both combined can be regarded as a closed system for all practical matters. Mathematically, the kinematic structure is given by the product $\mathcal{H}_{\text{sys}} \otimes \mathcal{H}_{\text{env}}$ or any Hilbert space isomorphic to it. For such an isolated system, the time evolution is governed by the usual postulates of quantum mechanics, that is the Schrödinger or the von Neumann equation for pure or mixed initial state, respectively. Since the environment's purpose is merely to restore a unitary time evolution, all relevant information about the system is encoded in the *reduced state* $\rho(t) = \text{Tr}_{\text{env}} \rho_{\text{tot}}(t)$ obtained by tracing over the environmental degrees of freedom. Formally, this amounts to assigning the expectation value

$$\langle A \rangle := \text{Tr}(\rho_{\text{tot}}(t)\, A \otimes I_{\text{env}}) = \text{Tr}_{\text{sys}}(\rho(t)\, A) \tag{1.1}$$

to each observable $A$ on $\mathcal{H}_{\text{sys}}$. The second part, namely that $\langle \cdot \rangle$ defines a genuine trace-class operator $\rho_t$ on $\mathcal{H}_{\text{sys}}$, follows under some additional regularity assumptions [5]. Although the total system-bath state is pure at any given time, the reduced state is not necessarily a pure-state projector. On the contrary, quantum entanglement caused by the interaction requires assigning a true mixture to the system—this makes the treatment of open quantum system so much harder compared to its classical counterpart.

Although the reduced state's time evolution is uniquely defined by the von Neumann equation for $\rho_{\text{tot}}(t)$ and Eq. (1.1), a dynamical equation purely in terms of $\rho(t)$, a *Master equation*, is more desirable for all practical purposes. In general, the derivation of a closed equation in $\rho(t)$ from the unitary system-bath evolution relies on quite severe approximations. A typical example is the *Redfield*-equation [6], which is based on the following physical assumptions: First, one starts with a initial product state $\rho_{\text{tot}}(0) = \rho(0) \otimes \rho_{\text{env}}$. By the weak-coupling or *Born*-approximation, this product

form with a fixed environmental state $\rho_{\text{env}}$ is preserved for all times. Furthermore, we assume that the dynamics of the environment proceed on a much smaller timescale compared to the system and any "memory"-effects are negligible small—this is the *Markov*-approximation However, because it is derived from a truncated perturbation expansion, the Redfield-master equation does not necessarily preserve all properties of a genuine density matrix.

A more robust approach based on similar physical assumptions, but more axiomatic in spirit has been elaborated by Linblad [29]: It is formulated purely in terms of propagators $\Lambda_t$ on the system's Hilbert space without making reference to a certain environment. The Born-Markov approximation is rephrased to the condition that the family of maps $(\Lambda_t)_{t \geq 0}$ constitute a quantum dynamical semi-group [2], namely $\Lambda_{s+t} = \Lambda_s \Lambda_t$. Provided the $\Lambda_t$ are completely-positive as well, the corresponding Master equation for the reduced state necessarily takes the Linblad form

$$\partial_t \rho_t = -\frac{\mathrm{i}}{\hbar}[H, \rho_t] + \frac{1}{2} \sum_n \left( [L_n \, \rho_t, L_n^\dagger] + [L_n, \rho_t \, L_n^\dagger] \right). \tag{1.2}$$

Here $H = H^\dagger$ is a self-adjoint operator and $L_n$ are Linbladians describing various irreversible channels [53].

no universally valid and tractable non-Markovian generalization of the Lindblad Master equation is known today. The projection formalism of Nakajima-Zwanzig provides a closed equation in the reduced state $\rho_t$ by separating relevant and irrelevant degrees of freedom in the von Neumann equation [6]. However, it includes non-Markovian effects by a memory-integral such that the evolution of $\rho(t)$ depends on all reduced states at times prior to $t$. This renders analytical or numerical solutions without further approximations virtually impossible.

A completely different approach to the dynamics of open quantum systems is the influence-functional formalism [14, 15]: Besides its strength in analytical calculations

## 1.2. Unravellings

## 1.3. Established Results and Subject of this Work

## 1.4. Outline

# 2. Non-Markovian Quantum State Diffusion

The description of open quantum systems in terms of diffusive stochastic differential equations has a long tradition [8, 19, 35]. At first, seen merely as a tool to unravel a given master equation of Lindblad type, it was realized later that they posses a strong microscopical foundation in terms of continuous measurements or memoryless quantum environments [3, 53].

The present work is based on a non-Markovian generalization, namely the non-Markovian quantum state diffusion (NMQSD), independently derived as an unravelling for the Feynman-Vernon influence functional in terms of stochastic propagators [46] and from the standard open-system-model [9], which we recall in Sect. 2.1. Following the lines of Diósi, Strunz and Gisin [10, 11, 48] we derive both, a linear and a numerically superior non-linear version of the NMSSE for zero temperature in Sect. 2.2 and 2.3, respectively. Section 2.4 is concerned with the question if our NMSSE has a physical interpretation or is merely a computational tool. Subsequently we drop the requirement of a zero temperature environment and show how to modify our approach to incorporate an initial thermal state. This chapter is concluded by the analytic treatment of an exactly solvable two-level system.

## 2.1. The Microscopical Model

It is the foremost goal of this work to obtain a dynamical description for an open-system's reduced state. Nevertheless, we introduce a full model of system and environment first, that is the bosonic and non-relativistic standard model of an open quantum system extensively studied for example in the book of Weiss [52]. There are three reasons for such a microscopical approach: On one hand, this serves the purpose to better understand the physical origin of macroscopical properties used to

characterize the environment later on. But more importantly, starting with a closed quantum system is the only strategy allowing us to derive of the NMSSE from first principles, namely the Schrödinger equation. As a last argument we mention that the reduced dynamics are greatly influenced by the choice of initial conditions. Especially, effects of entanglement on the system's time evolution are not well understood []—in what follows we ignore this point and always work with separable initial conditions.

As a starting point, we consider an environment consisting of a finite number $N$ of uncoupled harmonic oscillators[1]. A generalization to an infinite number can be carried out formally along the same lines, replacing sums by infinite series or even integrals; a different approach within our framework is presented later. The dynamics of both system and environment are then described by a unitary time evolution with Hamiltonian

$$H_{\text{tot}} = H \otimes \mathrm{I} + \mathrm{I} \otimes H_{\text{env}} + H_{\text{int}}, \tag{2.1}$$

where $H$ and $H_{\text{env}}$ are the free Hamiltonians of the system and the bath respectively and I denotes the identity on the appropriate Hilbert space. The latter is a sum over free harmonic oscillators $H_{\text{env}} = \sum_\lambda \omega_\lambda a_\lambda^\dagger a_\lambda$ expressed in bosonic ladder operators $a_\lambda$ and $a_\lambda^\dagger$ of the $\lambda^{\text{th}}$ mode with frequency $\omega_\lambda$. Treating a finite number of independent reservoirs poses no further difficulties and therefore is not elaborated in this section.

For the interaction between environment and system we confine ourselves to the case of linear coupling

$$H_{\text{int}} = \sum_\lambda g_\lambda^* \, L \otimes a_\lambda^\dagger + g_\lambda \, L^\dagger \otimes a_\lambda. \tag{2.2}$$

Here $L$ denotes the coupling operator in the system's Hilbert space and $g_\lambda \in \mathbb{C}$ the coupling strength of the $\lambda^{\text{th}}$ mode. In the field of condensed matter physics, typical models involve a coupling of an individual bath mode that scales inversely with the environment size [52], hence, the linear coupling in (2.2) seems reasonable for macroscopic large reservoirs. Also, the interaction of an electron with the electromagnetic field is described by a Hamiltonian (2.2) up to very high precision—leaving aside some extreme conditions [51]. But our framework is not restricted to such

---

[1] We use "environment", "reservoir" and "bath" interchangeably though the latter two suggest a large size compared to the system.
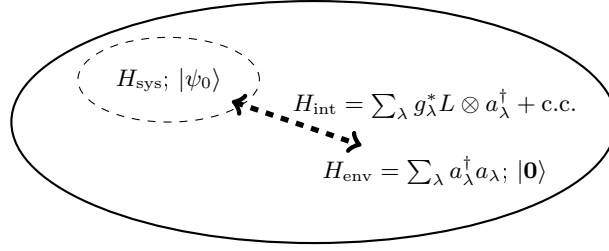
**Figure 2.1.:** Standard model of an open system immersed into a bosonic bath at zero temperature. The environmental oscillators with frequencies $\omega_\lambda$ are described in terms of ladder operators $a_\lambda$ and $a_\lambda^\dagger$. A coupling operator $L$ mediates the influence of the environment.

weak-coupling regimes, therefore, in such cases the linearity is imposed as another assumption.

Beside the full Hamiltonian, another important influence on the system's subdynamics is the initial state, specifically the initial entanglement between system and bath. Throughout this work we only consider product initial conditions, where the bath is in the vacuum state with respect to all $a_\lambda$

$$|\Psi_0\rangle = |\psi_0\rangle \bigotimes_\lambda |0_\lambda\rangle. \tag{2.3}$$

Such a choice is not as restrictive as it seems on first glance: In Sect. 2.5 we show how a thermal bath state can be mapped to this case. However, it is far from clear if the results of this work carry over to more general initial conditions, as the NMSSE and most strategies to solve it crucially depend on Eq. (2.3).

To absorb the free dynamics of the environment in time dependent creation and annihilation operators, we switch to the interaction picture with respect to $H_{\text{env}}$. Since the bath operators merely obtain an additional phase $\mathrm{e}^{\pm \mathrm{i}\omega_\lambda t}$, the transformed Hamiltonian from Eq. (2.4) reads[2]

$$H_{\text{tot}}(t) = H \otimes \mathrm{I} + \sum_\lambda \left( g_\lambda^* \mathrm{e}^{\mathrm{i}\omega_\lambda t} L \otimes a_\lambda^\dagger + g_\lambda \mathrm{e}^{-\mathrm{i}\omega t} L^\dagger \otimes a_\lambda \right). \tag{2.4}$$

---

[2]We refrain from introducing another label to distinguish between time-evolution pictures; in what follows we always work in the interaction picture.

Our choice of separable initial conditions with a vacuum bath state ensures that the reduced density operator remains unaffected under the change of time-evolution picture.

It is instructive to rewrite the last equation using the operator valued "force"

$$B(t) = \sum_\lambda g_\lambda a_\lambda \mathrm{e}^{-\mathrm{i}\omega_\lambda t}. \tag{2.5}$$

The total Hamiltonian then reads $H_{\mathrm{tot}}(t) = H \otimes \mathrm{I} + L \otimes B(t)^\dagger + L^\dagger \otimes B(t)$. From this equation it can already be seen that the complete action of the environment on the system is encoded in the operator $B(t)$. An important—and within our model the only—characteristic of them is the correlation function $\alpha(t-s) = \big\langle (B(t) + B(t)^\dagger)(B(s) + B(s)^\dagger)\big\rangle_\rho$, where $\langle \cdot \rangle_\rho$ denotes the exception value with respect to an arbitrary bath density matrix $\rho$. For a thermal state at temperature $T$, the correlation function can be calculated analytically [15]

$$\alpha_T(t-s) = \sum_\lambda |g_\lambda|^2 \left( \coth\left(\frac{\omega_\lambda}{2T}\right) \cos\omega_\lambda(t-s) - \mathrm{i}\sin\omega_\lambda(t-s) \right). \tag{2.6}$$

Introducing the spectral density $J(\omega) = \sum_\lambda |g_\lambda|^2 \delta(\omega - \omega_\lambda)$ and taking the limit $T \to 0$, Eq. (2.6) is written more concisely as

$$\alpha(t-s) = \langle B(t)B(s)^\dagger\rangle_0 = \int_0^\infty J(\omega)\mathrm{e}^{-\mathrm{i}\omega(t-s)}\,\mathrm{d}\omega, \tag{2.7}$$

provided all oscillator-frequencies $\omega_\lambda$ are positive. In other words, the zero-temperature correlation function is simply the (one-sided) Fourier transform of the spectral density. Since a genuine physical spectral density is real, we require admissible correlation functions to be hermitian $\alpha(-t) = \alpha(t)^*$.

Typical correlation functions of macroscopic systems decay exponentially on a timescale $\tau_{\mathrm{c}}$ called correlation time. The Markov limit $\tau_{\mathrm{c}} \to 0$ amounts to a completely memoryless time evolution and leads to the celebrated quantum dynamical semi-groups. On the other hand, a finite environment constitutes a purely oscillatory correlation function with $\tau_{\mathrm{c}} \to \infty$.

## 2.2. Linear NMSSE

The linear non-Markovian stochastic Schrödinger equation (NMSSE) derived in this section is an equivalent reformulation of the interaction-picture Schrödinger equation

$$\partial_t |\Psi_t\rangle = -\mathrm{i} H_{\mathrm{tot}}(t)|\Psi_t\rangle, \qquad |\Psi_0\rangle = |\psi_0\rangle \otimes |0\rangle, \tag{2.8}$$

corresponding to the model of the last section: As we elaborate in this section, expressing the bath degrees of freedom in the Bargmann Hilbert space of anti-holomorphic functions [4] provides a representation well suited to a stochastic interpretation. To this end we introduce the unnormalized coherent state $|z_\lambda\rangle = \exp(z_\lambda a_\lambda^\dagger)|0_\lambda\rangle$ for each mode with resolution of the identity for the environment

$$\mathrm{I} = \int \frac{\mathrm{e}^{-|\boldsymbol{z}|^2}}{\pi^N} |\boldsymbol{z}\rangle\langle\boldsymbol{z}| \, \mathrm{d}^{2N}z. \tag{2.9}$$

Here we employ the shorthand notation $|\boldsymbol{z}\rangle = \bigotimes_\lambda |z_\lambda\rangle$ and the "volume" integration measure for $N$ complex numbers $\mathrm{d}^{2N}z = \prod_\lambda \mathrm{d}\Re z_\lambda \, \mathrm{d}\Im z_\lambda$. Throughout this work the finite bath is often replaced by a continuum of oscillators; therefore we simply write $\mu(\mathrm{d}z) = \pi^{-N}\exp(-|\boldsymbol{z}|^2)\,\mathrm{d}^{2N}z$ and drop the explicit reference to $N$.

Equation (2.9) allows us to expand the full state in a time-independent environment basis

$$|\Psi_t\rangle = \int |\psi_t(\boldsymbol{z}^*)\rangle \otimes |\boldsymbol{z}\rangle \, \mu(\mathrm{d}z).$$

For the following derivation it is crucial to notice that the Bargmann transform $\boldsymbol{z} \mapsto \psi_t(\boldsymbol{z}^*)$ is an anti-holomorphic function with values in the system's Hilbert space $\mathcal{H}_{\mathrm{sys}}$. Naturally it is equivalent to any other representation of the full state $|\Psi_t\rangle$. As the coherent states are not orthogonal, but rather satisfy $\langle\boldsymbol{w}|\boldsymbol{z}\rangle = \exp(\sum_\lambda w_\lambda^* z_\lambda)$, the reduced density operator, obtained by tracing over the bath degrees of freedom, reads

$$\rho(t) = \mathrm{Tr}_{\mathrm{env}} |\Psi_t\rangle\langle\Psi_t| = \int |\psi_t(\boldsymbol{z}^*)\rangle\langle\psi_t(\boldsymbol{z}^*)| \, \mu(\mathrm{d}z). \tag{2.10}$$

After having established the kinematic structure, the next step is to rewrite the dynamical equation: The representation of the ladder operators follows from the usual rules $\langle\boldsymbol{z}|a_\lambda^\dagger = z_\lambda^*\langle\boldsymbol{z}|$ and $\langle\boldsymbol{z}|a_\lambda = \partial_{z_\lambda^*}\langle\boldsymbol{z}|$. These expressions, applied to Eq. (2.8), yield

the system-bath Schrödinger equation in the transformed space

$$\partial_t \psi_t(\boldsymbol{z}^*) = -\mathrm{i}H\psi_t(\boldsymbol{z}^*) - \mathrm{i}L\sum_\lambda g_\lambda^* \mathrm{e}^{-\mathrm{i}\omega_\lambda t} z_\lambda^* \, \psi_t(\boldsymbol{z}^*) - \mathrm{i}L^\dagger \sum_\lambda g_\lambda \mathrm{e}^{\mathrm{i}\omega_\lambda t} \frac{\partial \psi_t}{\partial z_\lambda}(\boldsymbol{z}^*). \quad (2.11)$$

Introducing an effective driving process like in Eq. (2.5)

$$Z_t^*(\boldsymbol{z}^*) = -\mathrm{i}\sum_\lambda g_\lambda^* \mathrm{e}^{-\mathrm{i}\omega_\lambda t} z_\lambda^* \quad (2.12)$$

allows us to combine the effect of the first bath-interaction term into a single multiplication operator—or process—for reasons explained in the next paragraph. A similar conversion works for the second term as well with the help of the functional chain rule $\frac{\partial}{\partial z_\lambda^*} = \int \frac{\partial Z_s^*}{\partial z_\lambda^*} \frac{\delta}{\delta Z_s^*} \, \mathrm{d}s$. Combined our new equation of motion, the non-Markovian stochastic Schrödinger equation, reads

$$\partial_t \psi_t = -\mathrm{i}H\psi_t + LZ_t^*\psi_t - L^\dagger \int_0^t \alpha(t-s) \frac{\delta \psi_t}{\delta Z_s^*} \, \mathrm{d}s. \quad (2.13)$$

This is the non-Markovian stochastic Schrödinger equation (NMSSE) first derived by Diósi and Strunz [11]. As we show in Sect. 2.4, the integral boundaries arise by virtue of the initial conditions (2.3), but the basic idea is simple: By definition of our processes (2.12) an initial state $|\psi_0\rangle \otimes |0\rangle$ translates to an initial $\psi_0$ that is completely independent of the noise. Then, causality implies that $\psi_t$ can only depend on $Z_s^*$ for $0 \le s \le t$.

Up to this point we have merely rewritten the original Schrödinger equation (2.8) to an equivalent form: The original system-bath product Hilbert space $\mathcal{H}_{\mathrm{sys}} \otimes \mathcal{H}_{\mathrm{env}}$ is simply replaced by a Hilbert space of $\mathcal{H}_{\mathrm{sys}}$-valued functions holomorphic in $Z_t^*$. A different attitude is quite fruitful, especially with a numerical solution of the NMSSE in mind: Equation (2.10) can be rewritten as $\rho_t = \mathbb{E}(|\psi_t\rangle\langle\psi_t|)$, where $\mathbb{E}$ denotes the average over $\mu(\mathrm{d}z) = \pi^{-N}\exp(-|\boldsymbol{z}|^2)\,\mathrm{d}^{2N}z$. Put differently, the reduced density matrix $\rho_t$ arises from averaging over stochastic pure state projectors $|\psi_t(\boldsymbol{z}^*)\rangle\langle\psi_t(\boldsymbol{z}^*)|$ with Gaussian weight $\mu(\mathrm{d}z)$. Hence, we regard Eq. (2.13) as a stochastic differential equation for individual realisations $\psi_t(\boldsymbol{z}^*)$. We refer to the latter either as system state relative to $|\boldsymbol{z}\rangle$ or, in the spirit of the stochastic Schrödinger equations emerging

from continuous measurement theory [8], as quantum trajectory.

In this approach, the influence of the bath is implemented as classical stochastic process $Z_t^*$ defined by the concrete version (2.12) and the underlying probability measure $\mu$. It is a complex Gaussian process, uniquely characterized by its expectation value and covariances

$$\mathbb{E}\, Z_t = 0, \quad \mathbb{E}\, Z_t Z_s = 0, \quad \text{and} \quad \mathbb{E}\, Z_t Z_s^* = \alpha(t - s), \qquad (2.14)$$

where $\alpha$ is the zero-temperature correlation function (2.7) for $J(\omega) = \sum_\lambda |g_\lambda|^2 \delta(\omega - \omega_\lambda)$. By virtue of the initial conditions, $\psi_t$ depends on $z^*$ only through the noise process; thus we can drop the coherent state labels and simply write $\psi_t(Z^*)$ denoting the trajectory corresponding to the realization $Z_t^*(z^*)$. To go one step further, we regard Eq. (2.14) as the defining properties of $Z_t^*$ without any reference to the microscopic model. It is this alternative point of view that makes the NMSSE-approach so powerful: The entire influence of the environment is encoded in a complex function $\alpha$, which acts both as correlation function for the driving noise $Z_t^*$ and as memory kernel for the damping term. A generalization to an arbitrary number of bath-oscillators is now straightforward: Replacing $\alpha$ by any admissible bath correlation function allows a unified treatment of arbitrary bosonic environments.

Except in the limit $\alpha(t) \sim \delta(t)$, elaborated in the next paragraph, the noise process $Z_t^*$ is correlated for different times. This non-Markovian behavior, which makes a complete understanding of the dynamics highly desirable for application but also considerably harder, shows up in the equation of motion (2.13) as well. The memory integral contains the functional derivative over the whole timespan and therefore takes the complete history of $\psi_t(Z^*)$ into account. In its own right the derivative is just as problematic: Since its computation requires not only the single realisation $Z_t^*$, but in some sense all adjacent ones as well, it seems questionable to regard the NMSSE (2.13) as a genuine stochastic differential equation [17]. Even from the purely pragmatic point of view, both kinds of non-local behavior complicate a direct numerical simulation of the NMSSE—or even make it completely impracticable. Nevertheless, there are two quite distinct solutions to this problem as shown in Sect. 2.2.1 and Chap. 3.

## 2.2.1. Convolutionless Formulation

As a cure for the non-locality issues, Diósi, Gisin, and Strunz [10] proposed the powerful $O$-Operator substitution: It is based on the additional assumption, that one may replace the functional derivative by a system operator $O$, which only depends on the realisation of $Z^*$ itself

$$\frac{\delta\psi_t(Z^*)}{\delta Z_s^*} = O(t, s, Z^*)\psi_t(Z^*). \tag{2.15}$$

Besides getting rid of the derivative, this substitution enables us to derive a convolutionless form of our NMSSE (2.13)

$$\partial_t\psi_t = -\mathrm{i}H\psi_t(Z^*) + LZ_t^*\psi_t(Z^*) - L^\dagger\bar{O}(t, Z^*)\psi_t(Z^*) \tag{2.16}$$

with the time-local operator

$$\bar{O}(t, Z^*) := \int_0^t \alpha(t - s)O(t, s, Z^*)\,\mathrm{d}s. \tag{2.17}$$

Conclusively, Eq. (2.16) turns into a genuine stochastic differential equation for the trajectory $\psi_t(Z^*)$, but in the much smaller Hilbert space of the system. This makes it exceptionally well suited for dealing with infinite sized environments numerically, provided the $\bar{O}$-operator is known. Depending on the validity of the $O$-substitution the corresponding convolutionless NMSSE (2.16) might be as accurate as the original microscopic equation of motion (2.8).

In general one proceeds as follows [10]: From the consistency condition

$$\partial_t \frac{\delta\psi_t(Z^*)}{\delta Z_s^*} = \frac{\delta}{\delta Z_s^*}\partial_t\psi_t(Z^*) \tag{2.18}$$

supplied with initial value

$$O(s, s, Z^*) = L \tag{2.19}$$

we derive an equation of motion for $O(t, s, Z^*)$. It still contains the functional derivative, but is converted to a system of coupled, deterministic equations using a power

series ansatz

$$O(t, s, Z^*) = \sum_{n=0}^{\infty} \int_0^t \ldots \int_0^t O_n(t, s, \nu_1, \ldots, \nu_n) \, \mathrm{d}\nu_1 \ldots \nu_n. \qquad (2.20)$$

For a few simple systems—for example the Jaynes-Cummings model presented in Sect. 2.6 or its higher dimensional generalizations [26]—an exact analytic expression for $O(t, s, Z^*)$ is known. Nevertheless, most treatments rely on approximation schemes, for example a perturbation expansion for small coupling parameter or almost-Markovian environments [55]. Also a closely related hierarchy of $\bar{O}$-operators provides an efficient numerical algorithm similar in concept to the main result of this work.

### 2.2.2. Markov Limit

Markovian dynamics constitute an important limit in the description of open quantum systems. In this section we show how a bath correlation function with vanishing correlation time, namely $\alpha(t) = \gamma \delta(t)$, transforms the NMSSE into the linear, diffusive stochastic Schrödinger equation **??**, thus establishing the link to the well-known Markovian theory.

The vacuum initial conditions $\frac{\delta \psi_0}{\delta Z_s^*} = 0$ with $s \in \mathbb{R}$ imply for an arbitrary bath correlation function

$$\frac{\delta \psi_t}{\delta Z_t^*} = \frac{1}{2} \, L \psi_t \qquad (t > 0) \text{???} \qquad (2.21)$$

as we show now directly from the equations of motion[3]

It is clear from its derivation that the NMSSE describes a unitary time evolution. Therefore it can be solved formally using the Dyson series

$$\psi_t(Z^*) = \sum_{n=0}^{\infty} (-\mathrm{i})^n \int_0^t \mathrm{d}t_1 \int_0^{t_1} \mathrm{d}t_2 \ldots \int_0^{t_{n-1}} \mathrm{d}t_n \, H_{\text{tot}}(t_1) \ldots H_{\text{tot}}(t_n) \, \psi_0, \qquad (2.22)$$

---

[3] Equation (2.21) deviates from the acquainted result (2.19) by a factor $\frac{1}{2}$, as the latter is derived without any reference to the functional derivative. Instead, the $O$-operator is already introduced in the microscopical model using the Heisenberg time evolution picture for the annihilation operator $a_\lambda$ [47]. Therefore, the substitution Eq. (2.15) does not hold for $s = t$. However, this is insignificant for the integrated operator (2.17).

where $H_{\text{tot}}(t)$ is the reformulation of (2.4) given by

$$-\mathrm{i}H_{\text{tot}}(t) = -\mathrm{i}H + LZ_t^* - L^\dagger \int_{-\infty}^{\infty} \mathrm{d}s\, \alpha(t-s)\frac{\delta}{\delta Z_s^*}.$$

Throughout this work we often use the shorthand notation $\mathcal{D}_t = \int \mathrm{d}s\, \alpha(t-s)\frac{\delta}{\delta Z_s^*}$ for the last term. Recall that the bounded integral domain in the NMSSE arises by virtue of the initial conditions—no such restriction applies to $\mathcal{D}_t$.

The functional derivative $\frac{\delta}{\delta Z_s^*}$ of $H_{\text{tot}}(t)$ gives a single contribution $\mathrm{i}\delta(t-s)L$ due to $\frac{\delta Z_t^*}{\delta Z_s^*} = \delta(t-s)$. This allows us to calculate $\frac{\delta \psi_t}{\delta Z_t^*}$ order by order in Eq. (2.22): With vanishing derivative of $\psi_0$ as imposed by the initial conditions, we obtain for the first order

$$\frac{\delta}{\delta Z_t^*} \int_0^t \mathrm{d}t_1\, (-\mathrm{i})H_{\text{tot}}(t_1)\psi_0 = \int_0^t \mathrm{d}t_1\, \delta(t-t_1)L\psi_0 = \frac{1}{2}\, L\psi_0$$

and similarly for the second order

$$\frac{\delta}{\delta Z_t^*} \int_0^t \mathrm{d}t_1 \int_0^{t_1} \mathrm{d}t_2\, (-\mathrm{i})^2 H_{\text{tot}}(t_1)H_{\text{tot}}(t_2)\psi_0$$
$$= \int_0^t \mathrm{d}t_1 \int_0^{t_1} \mathrm{d}t_2\, (-\mathrm{i})\Big(\delta(t-t_1)LH_{\text{tot}}(t_2) + \delta(t-t_2)H_{\text{tot}}(t_1)L\Big)\psi_0$$
$$= \frac{1}{2}\, L \int_0^t \mathrm{d}t_2\, (-\mathrm{i})H_{\text{tot}}(t_2)\psi_0$$

To justify the second identity, notice that $\delta(t-t_2)$ contributes only if $t_1 \geq t$, since otherwise the singular point $t$ of the $\delta$-function lies outside the integration domain. However, this condition is only satisfied with vanishing weight under the $t_1$ integral, as the latter is confined to $[0,t]$. The same scheme carries over to all higher orders in Eq. (2.22), leading to Eq. (2.21).

Let us return to the Markov limit of our NMSSE: By virtue of the singular correlation function $\alpha(t) = \gamma\delta(t)$, the memory integral reduces to a time-local form

$$\mathcal{D}_t = \int \delta(t-s)\frac{\delta}{\delta Z_s^*}\,\mathrm{d}s = \gamma\frac{\delta}{\delta Z_t^*}$$

as it is expected from a memoryless environment. Combined with Eq. (2.21), this

leads to a simple stochastic differential equation

$$\partial_t \psi_t(Z^*) = -\mathrm{i}H\psi_t(Z^*) + LZ_t^*\psi_t(Z^*) - \frac{\gamma}{2}L^\dagger L\psi_t(Z^*), \qquad (2.23)$$

driven by a complex White Noise $Z_t$ with $\mathbb{E}Z_tZ_s^* = \gamma\delta(t-s)$. In a formally exact fashion, the equation above should be written as

$$\mathrm{d}\psi_t = (-\mathrm{i}H\psi_t - \frac{\gamma}{2}L^\dagger L\psi_t)\,\mathrm{d}t + \sqrt{\gamma}L\psi_t\,\mathrm{d}\xi_t^* \qquad (2.24)$$

with the increments of a standard complex Brownian motion $\mathrm{d}\xi_t$. It is well known that, seen as an ordinary differential equation, Eq. (2.24) is problematic since $\xi_t$ is not differentiable with respect to time. To define the solution $\psi_t$ uniquely we need to specify an appropriate interpretation of the stochastic differential equation: Since we treat the original NMSSE—at least for a finite environment—in Euler-calculus, its Markovian limit should be interpreted in Stratonovich's sense [34]. However, in our case the Itō- and Stratonovich form agree since $\mathbb{E}\xi_t\xi_s = 0$ [20].

## 2.2.3. Equivalent Master Equations

Although this work is entirely dedicated to the NMSSE, for the sake of completeness we provide the connection to the customary Master equations in this section. The latter are formulated in terms of reduced density operators, which we recover from the trajectories by averaging over the pure states projectors $P_t = |\psi_t(Z^*)\rangle\langle\psi_t(Z^*)|$. But the $O$-operator substitution is essential for clarifying the connection to the master equations commonly used in the theory of open quantum systems as well. For certain systems this can be done analytically utilizing the $O$-operator introduced in Sect. 2.2.1. As a simple example, we focus on models with a $Z^*$ independent $\bar{O}$-operator, though the general case is treated along the same lines [55, 56]. We start from the pure-state projectors' equations of motion

$$\partial_t P_t = -\mathrm{i}[H, P_t] + Z_t^* L P_t - L^\dagger \bar{O}(t)P_t + Z_t P_t L^\dagger - P_t\bar{O}(t)^\dagger L. \qquad (2.25)$$

After averaging over the bath degrees of freedom, these yield a closed evolution equation for $\rho_t$ only if we can restate the terms containing $Z_t$ and $Z_t^*$ in a noise-independent

manner. This can be done with the help of Novikov's formula [33]

$$\mathbb{E}\left(Z_t P_t\right) = \mathbb{E}\left(\int \mathrm{d}s\alpha(t-s)\frac{\delta}{\delta Z_s^*}P_t\right), \tag{2.26}$$

which amounts to a partial integration under the Gaussian integrals (2.10).

The right hand side of Novikov's formula is simplified further using the $O$-operator substitution once again. Since $|\psi_t\rangle$ is analytical in $Z_s^*$, and accordingly $\langle\psi_t|$ analytical in $Z_s$, the derivative is further simplified to

$$\frac{\delta}{\delta Z_s^*}\left(|\psi_t(Z^*)\rangle\langle\psi_t(Z^*)|\right) = \left(\frac{\delta}{\delta Z_s^*}|\psi_t(Z^*)\rangle\right)\langle\psi_t(\boldsymbol{z})| = O(t,s)|\psi_t(Z^*)\rangle\langle\psi_t(Z^*)|.$$

Averaging over the equations of motion for the pure state projectors (2.25) finally gives the master equation for the reduced density matrix $\rho_t$

$$\partial_t\rho_t = -\mathrm{i}[H, \rho_t] + [L, \rho_t\bar{O}(t)^\dagger] + [\bar{O}(t)\rho_t, L^\dagger]. \tag{2.27}$$

This expression closely resembles the well-known Lindblad master equation (1.2) for Markovian open quantum systems, but involves time-dependent Lindbladians. As elaborated in  Sect. 2.2.2, the $\bar{O}$-operator reduces to $\bar{O}(t) = \frac{\gamma}{2}L$ for a Markovian environment—thus the master equation (2.27) derived from the NMSSE reproduces the correct limit.

## 2.3. Nonlinear NMSSE

From a fundamental point of view, the linear non-Markovian stochastic Schrödinger equation (2.13) is fascinating in its own right. It provides a unified description of arbitrary structured environments and admits a figurative interpretation presented in  Sect. 2.4. But, there is a major drawback when it comes to practical application in terms of Monte-Carlo simulations: Recall that the reduced density matrix $\rho_t$ is obtained by averaging over individual pure state projectors $|\psi_t(Z^*)\rangle\langle\psi_t(Z^*)|$. The quality of such a scheme is drastically reduced if there are few highly peaked contributions [12]. As demonstrated exemplary for the spin-boson model in  Sect. 3.4.1, the NMSSE displays such a behavior: The norm of most trajectories goes to zero as $t \to \infty$ due to ever growing entanglement with the environment. To recover a

unitary time evolution for system and bath, that is $\mathbb{E}\left(\langle\psi_t|\psi_t\rangle\right) = \langle\Psi_t|\Psi_t\rangle = 1$, in a Monte-Carlo simulation, the average has to taken over many trajectories in order to catch a few with significant contribution. This requires an insurmountable sample size for certain parameter regimes as we show for the exemplary Spin-Boson model.

Of course, we have just described the problem of importance sampling in statistics; for its solution let us return to the microscopical model from Sect. 2.1. The key observation is that the average yielding the reduced density operator (2.10) is not unique: A change in the integration measure $\mu(\mathrm{d}z)$ can be compensated using a Girsanov transformation on the quantum trajectories $\psi_t(Z^*)$. We use this fact to rewrite the density operator as an average over normalized states

$$\rho_t = \int \frac{\mathrm{d}^{2N}z}{\pi^N}\,\mathrm{e}^{-|\boldsymbol{z}|^2}\langle\psi_t(\boldsymbol{z}^*)|\psi_t(\boldsymbol{z}^*)\rangle\,\frac{|\psi_t(\boldsymbol{z}^*)\rangle\langle\psi_t(\boldsymbol{z}^*)|}{\langle\psi_t(\boldsymbol{z}^*)|\psi_t(\boldsymbol{z}^*)\rangle} \tag{2.28}$$

$$= \int \mathrm{d}^{2N}z\,Q_t(\boldsymbol{z},\boldsymbol{z}^*)\,\frac{|\psi_t(\boldsymbol{z}^*)\rangle\langle\psi_t(\boldsymbol{z}^*)|}{\langle\psi_t(\boldsymbol{z}^*)|\psi_t(\boldsymbol{z}^*)\rangle}, \tag{2.29}$$

now with a time dependent density function under the integral

$$Q_t(\boldsymbol{z},\boldsymbol{z}^*) = \frac{\mathrm{e}^{-|\boldsymbol{z}|^2}}{\pi^N}\,\langle\psi_t(\boldsymbol{z}^*)|\psi_t(\boldsymbol{z}^*)\rangle = \frac{\mathrm{e}^{-|\boldsymbol{z}|^2}}{\pi^N}\,\langle\boldsymbol{z}|\,\mathrm{Tr}_{\mathrm{sys}}\left(|\Psi_t\rangle\langle\Psi_t|\right)|\boldsymbol{z}\rangle. \tag{2.30}$$

Remarkably the latter coincides with the Husimi- or Q-function[4] of the environmental oscillators [43]. Being non-negative and normalized to unity $\int Q(\boldsymbol{z},\boldsymbol{z}^*)\,\mathrm{d}z = 1$ makes the Husimi-function a genuine (quasi-)probability distribution on phase space. In this representation, $|z\rangle$ resembles a wave packet localized around $z = (q + \mathrm{i}\,p)/\sqrt{2}$, thus, there is a well defined correspondence between coherent state labels $z$ and the canonical variables $(q,p)$. With Eq. (2.28), we conclude that the norm of a trajectory $\psi_t(\boldsymbol{z}^*)$ determines the probability to find the environment in a quantum state localized in the vicinity of a point $(\boldsymbol{q},\boldsymbol{p})$ in phase space. So, instead of using a fixed environmental basis $|\boldsymbol{z}\rangle$ to expand the full state $|\Psi_t\rangle$ we can incorporate the dynamics of the environment in a comoving coherent state basis.

Making use of the microscopic Hamiltonian (2.11) and the analyticity of $\psi_t(\boldsymbol{z}^*)$ in $\boldsymbol{z}^*$, that is $\partial_{z_\lambda}|\psi_t(\boldsymbol{z}^*)\rangle = 0$, we obtain an equation of motion, which closely resembles

---

[4]We point out that the Husimi function is usually defined in terms of normalized coherent states, hence, there is an additional factor $\exp(-|z_\lambda|^2)$ for each oscillator in our notation.

a Liouville equation

$$\partial_t Q_t(\boldsymbol{z}, \boldsymbol{z}^*) = -\sum_\lambda \partial_{z_\lambda^*} \big( \mathrm{i} g_\lambda \mathrm{e}^{-\mathrm{i}\omega_\lambda t} \langle L^\dagger \rangle_t Q_t(\boldsymbol{z}, \boldsymbol{z}^*) \big) - \text{c.c.} \tag{2.31}$$

Clearly, it contains the full influence of the system due to the quantum average

$$\langle L^\dagger \rangle_t = \frac{\langle \psi_t(\boldsymbol{z}^*) | L^\dagger | \psi_t(\boldsymbol{z}^*) \rangle}{\langle \psi_t(\boldsymbol{z}^*) | \psi_t(\boldsymbol{z}^*) \rangle}.$$

Just like its counterpart from classical mechanics, Eq. (2.31) is solved using the method of characteristics. The corresponding drift velocities are given by

$$\dot{z}_\lambda^*(t) = \mathrm{i} g_\lambda \mathrm{e}^{-\mathrm{i}\omega_\lambda t} \langle L^\dagger \rangle_t. \tag{2.32}$$

We denote the corresponding flow[5] by $\boldsymbol{\phi}_t^*$, or, using the more common notation, $z_\lambda^*(t) = \phi_{\lambda,t}^*(z_\lambda^*)$ with initial conditions $z_\lambda^*(0) = \phi_{\lambda,0}^*(z_\lambda^*) = z_\lambda^*$. Equation (2.32) admits the following interpretation: If we start with a total state $|\psi_t(\boldsymbol{z}^*)\rangle \otimes |\boldsymbol{z}\rangle$ of system and environment at time $t$, then the most relevant contribution to the full state at $t + \Delta t$ corresponds to the coherent state $|\boldsymbol{z} + \dot{\boldsymbol{z}}(t)\Delta t\rangle$. For this reason, we should expand $|\Psi_t\rangle$ with respect to $|\boldsymbol{z}(t)\rangle$ instead of a fixed basis in order to capture the dominant proportion and avoid propagating states irrelevant for the final average.

It is the method of characteristics' essential point that the flow $\boldsymbol{\phi}_t$ yields a solution of Eq. (2.31) by

$$Q_t(\boldsymbol{z}, \boldsymbol{z}^*) = \int \mathrm{d}^{2N} z_0 \, Q_0(\boldsymbol{z}_0, \boldsymbol{z}_0^*) \, \delta(\boldsymbol{z} - \boldsymbol{\phi}_t(\boldsymbol{z}_0)) \, \mathrm{d}^{2N}, \tag{2.33}$$

where $\delta(\boldsymbol{z} - \boldsymbol{z}') = \prod_\lambda \delta(\Re(z_\lambda - z_\lambda'))\delta(\Im(z_\lambda - z_\lambda'))$. Our initial product state $|\Psi_0\rangle = |\psi_0\rangle \otimes |\boldsymbol{0}\rangle$ combined with Eq. (2.30) yields the Husimi-function at $t = 0$ exactly as the original Gaussian weight $Q_0(\boldsymbol{z}, \boldsymbol{z}^*) = \pi^{-N}\mathrm{e}^{-|\boldsymbol{z}|^2}$ for a time-independent coherent state basis. Therefore, Eq. (2.33) finally reduces Eq. (2.28) to the sought-after average over normalized trajectories, but now with a time-independent probability

---

[5]In the following, we do not indicate the flow's non-holomorphic dependence on $\boldsymbol{z}^*$, caused by the expectation value of $L^\dagger$ in Eq. (2.32), explicitly, because we consider $\boldsymbol{\phi}_t^*$ as a function of the initial coherent state label $\boldsymbol{z}^*$ and the corresponding trajectory $\psi_t(\boldsymbol{z}^*)$.

measure

$$\rho_t = \int \frac{\mathrm{d}^{2N}z}{\pi^N} \, \mathrm{e}^{-|\boldsymbol{z}|^2} \, \frac{|\psi_t(\boldsymbol{\phi}_t^*(\boldsymbol{z}^*))\rangle\langle\psi_t(\boldsymbol{\phi}_t^*(\boldsymbol{z}^*))|}{\langle\psi_t(\boldsymbol{\phi}_t^*(\boldsymbol{z}^*))|\psi_t(\boldsymbol{\phi}_t^*(\boldsymbol{z}^*))\rangle} = \mathbb{E}\left(\frac{|\tilde{\psi}_t\rangle\langle\tilde{\psi}_t|}{\langle\tilde{\psi}_t|\tilde{\psi}_t\rangle}\right). \tag{2.34}$$

Here, we have introduced relative states $\tilde{\psi}_t(\boldsymbol{z}^*) = \psi_t(\boldsymbol{\phi}_t(\boldsymbol{z}^*))$ correspondig to the comoving coherent basis[6].

Of course, a practical application of Eq. (2.34) in a Monte-Carlo calculation crucially depends upon whether a closed equation of motion for $\tilde{\psi}_t$ exists. Remarkably, the latter satisfy a nonlinear version of our convolutionless NMSSE (2.16) as we show now starting from

$$\partial_t(\psi_t \circ \boldsymbol{\phi}_t^*) = \partial_t \psi_t \circ \boldsymbol{\phi}_t^* + \sum_\lambda (\partial_{z_\lambda^*} \psi_t \circ \boldsymbol{\phi}_t^*) \cdot (\partial_t \phi_{t,\lambda}^*). \tag{2.35}$$

The flow $\boldsymbol{\phi}_t^*$ in the first term amounts to evaluating the original equation of motion at the comoving coherent state $\boldsymbol{z}(t)$. Using its integral form

$$\phi_{t,\lambda}^*(z_\lambda^*) = z_\lambda^* + \mathrm{i}g_\lambda \int_0^t \exp(-\mathrm{i}\omega_\lambda s)\langle L^\dagger\rangle_s \, \mathrm{d}s \tag{2.36}$$

plugged into the microscopic version of the process (2.12) yields a shifted stochastic driving force

$$\tilde{Z}_t^*(\boldsymbol{z}^*) := Z_t^*(\boldsymbol{\phi}_t^*(\boldsymbol{z}^*)) = Z_t^*(\boldsymbol{z}^*) + \int_0^t \alpha(t-s)^*\langle L^\dagger\rangle_s \, \mathrm{d}s. \tag{2.37}$$

Since the $O$-operator substitution ensures that the equation of motion for $\psi_t$ is local with respect to $Z^*$, the first summand on the left hand side of Eq. (2.35) is obtained replacing $Z_t^*$ by $\tilde{Z}_t^*$ in the convolutionless NMSSE.

For the second summand, which accounts for the intrinsic time dependence of the

---

[6]It is more common in the literature to introduce normalized trajectories $\psi_t' = \tilde{\psi}_t/|\tilde{\psi}_t|$ directly without any reference to $\tilde{\psi}_t$. In this work however, the interim state $\tilde{\psi}_t$ plays a particularly important role for the hierarchical equations of motion and is therefore designated explicitly.

shifted coherent states, we utilize the functional chain rule once again

$$\sum_\lambda \frac{\partial \phi_{t,\lambda}^*}{\partial t}(z_\lambda^*) \cdot \frac{\partial \psi_t}{\partial z_\lambda^*}(\phi_t^*(\boldsymbol{z}^*)) = \mathrm{i} \sum_\lambda g_\lambda \mathrm{e}^{-\mathrm{i}\omega_\lambda t} \langle L^\dagger \rangle_t \frac{\partial \psi_t}{\partial z_\lambda^*}(\phi_t^*(\boldsymbol{z}^*))$$

$$= \langle L^\dagger \rangle_t \int_0^t \alpha(t-s) \frac{\delta \psi_t}{\delta Z_s^*}(\phi_t^*(\boldsymbol{z}^*)) \, \mathrm{d}s$$

$$= \langle L^\dagger \rangle_t \bar{O}(t, \tilde{Z}^*) \tilde{\psi}_t(\tilde{Z}^*),$$

where the last line reflects the definition of the $\bar{O}$-operator in Eqs. (2.15) and (2.17). Both terms of (2.35) combined yield the desired equation for $\tilde{\psi}_t$

$$\partial_t \tilde{\psi}_t = -\mathrm{i} H \tilde{\psi}_t + L \tilde{Z}_t^* \tilde{\psi}_t - (L^\dagger - \langle L^\dagger \rangle_t) \bar{O}(t, \tilde{Z}^*) \tilde{\psi}_t. \tag{2.38}$$

Although $\tilde{\psi}_t$ allows taking the average over normalized states, its equation of motion (2.38) does not preserve normalization over time. This can be achieved by adding further nonlinear terms: Considering trajectories $|\psi_t'(\tilde{Z}^*)\rangle = |\tilde{\psi}_t(\tilde{Z}^*)\rangle / |\tilde{\psi}_t(\tilde{Z}^*)|$ it is straightforward to derive the corresponding equation of motion [10]

$$\partial_t \psi_t' = -\mathrm{i} H \psi_t' + (L - \langle L \rangle_t) \tilde{Z}_t^* \psi_t'$$

$$- \left( (L^\dagger - \langle L^\dagger \rangle_t) \bar{O}(t, \tilde{Z}^*) - \left\langle (L^\dagger - \langle L^\dagger \rangle_t) \bar{O}(t, \tilde{Z}^*) \right\rangle_t \right) \psi_t', \tag{2.39}$$

where the quantum average $\langle \cdot \rangle_t$ is taken with respect to $\psi_t'$. Once again, the Markov-limit amounts to $\bar{O}(t, \tilde{Z}^*) = \frac{1}{2} L$ and replacing the noise process $Z_t^*$ by a complex White Noise. Thus, we obtain the well-known nonlinear unravelling of a Lindblad master equation [3].

As mentioned in the motivation, the nonlinear equations should be given precedence over the linear version when it comes to Monte-Carlo simulation. Although it requires propagating a new time-nonlocal, scalar quantity, namely $\langle L^\dagger \rangle_s$ for $0 \leq s \leq t$ in the shifted noise $\tilde{Z}_t^*$, the improved convergence with respect to the number of realizations compensates by far the additional computational demands.

## 2.4. Interpretation of NMSSE

In contrast to classical mechanics, assigning a reduced pure state to an open quantum system fails in general. Due to entanglement with the environment built up by interaction, the reduced state is described consistently only by a mixed state. However, quantum trajectories obtained as solutions of a linear or nonlinear Markovian stochastic Schrödinger equation are more than simply a convenient tool for calculations: These arise for example as trajectories of post-measurement pure states conditioned on a time-continuous measurement outcome [3,8], because the interaction with a measurement apparatus destroys system-environment entanglement.

The question, whether the NMSSE investigated in this work admits a similar interpretation, has been answered negative for a large class of models only recently: Krönke and Strunz [27] derived a consistency condition necessary for a measurement interpretation of the linear, convolutionless NMSSE with an $O$-operator that depends at most linearly on the noise process. This condition is violated by all exemplary systems they studied, except in the Markov limit $\alpha(t) \sim \delta(t)$.

We now present a different, less practical and more figurative interpretation of the linear NMSSE (2.13). The main goal is to establish the NMSSE as an alternative description for the unitary system-bath time evolution in terms of a "generalized environment". At first we state the Hilbert space used in the description:

<span style="color:red">COMPLETE</span>

## 2.5. Finite Temperature Theory

Until now, we were only concerned with the temperature zero theory, which is characterized by an initial product state with the environment in the vacuum state $|\Psi_0\rangle = |\psi_0\rangle \otimes |\mathbf{0}\rangle$. It translates into our NMSSE-framework as the demand of vanishing functional derivatives $\frac{\delta\psi_0}{\delta Z_s^*} = 0$ for arbitrary $s$ at $t = 0$. This property ensures the bounded integral domain of the functional derivative, which on the other hand is crucial for a causal interpretation in terms of time-oscillators. Also, the $O$-operator substitution as well as the hierarchical equations of motion depend on the temperature-zero assumption. In order to treat a thermal environment at arbitrary temperature, we devise a method that maps to the vacuum initial conditions.

Let us consider an initial product, where the bath assumes a Gibbs state $\rho(\beta) = Z^{-1} e^{-\beta H_{\text{env}}}$; more precisely

$$\rho_0 = |\psi_0\rangle\langle\psi_0| \otimes \rho(\beta) \tag{2.40}$$

with the bath partition function $Z = \text{Tr}\, e^{-\beta H_{\text{env}}}$ at inverse temperature $\beta = T^{-1}$. We cannot drop the requirement of separable initial state, however, Eq. (2.40) is a good approximation for some more realistic settings—see for example Chap. 4.

The thermo-field approach [] is based on the simple trick that a thermal state $\rho(\beta)$ can be expressed as vacuum in an enlarged environment, doubling the degrees of freedom. It is favored over other methods in the application to NMQSD since it preserves the structure of the equation of motion. Additionally, it constitutes a consistent way to include negative frequency oscillators in the environment, which on the other hand are required for the bath correlation function used to derive our hierarchy. The last point is further elaborated in Sect. 3.3. In the course of this section we follow the more detailed accounts of Yu and Strunz [47,54].

The main idea is to introduce a second fictitious bath of oscillators $\mathcal{B}$, which is independent from the physical environment $\mathcal{A}$ and does not interact with the system. Expressing its degrees of freedom in ladder operators $b_\lambda$ and $b_\lambda^\dagger$ gives us the new Hamiltonian in the Schrödinger picture

$$H_{\text{tot}} = H \otimes \text{I} + \sum_\lambda (g_\lambda^* L \otimes a_\lambda^\dagger + g_\lambda L^\dagger \otimes a_\lambda) + \text{I} \otimes \sum_\lambda \omega_\lambda(a_\lambda^\dagger a_\lambda - b_\lambda^\dagger b_\lambda). \tag{2.41}$$

Although the corresponding eigen-energies are not bounded from below due to negative frequencies of the fictitious oscillators, there are no stability problems since the latter do not interact with the physical degrees of freedom. For the same reason, the reduced dynamics obtained from Eq. (2.41) are identical to the original microscopical model (2.4), provided there is no initial entanglement of $\mathcal{B}$ with the system. Both yield equal reduced density matrices provided we choose an initial state $\tilde{\rho}$ for environments $\mathcal{A}$ and $\mathcal{B}$ that reproduces Eq. (2.40) after tracing over the unphysical degrees of freedom, that is

$$\text{Tr}_{\mathcal{B}}\, \tilde{\rho} = \rho(\beta). \tag{2.42}$$

Here, $\mathrm{Tr}_{\mathcal{B}}$ denotes the partial trace with respect to the fictitious degrees of freedom.

Remarkably, a solution $\tilde{\rho}$ of Eq. (2.42) is given by a pure state projector on a vacuum state with respect to new annihilation operators $A$, $B$. They are connected to the old ladder operators by a temperature dependent Bogoliubov transformation

$$A_\lambda = \sqrt{\bar{n}_\lambda + 1}\, a_\lambda + \sqrt{\bar{n}_\lambda}\, b_\lambda^\dagger$$
$$B_\lambda = \sqrt{\bar{n}_\lambda}\, a_\lambda^\dagger + \sqrt{\bar{n}_\lambda + 1}\, b_\lambda,$$

with $\bar{n}_\lambda = (\exp(\beta\omega_\lambda) - 1)^{-1}$ denoting the mean thermal occupation number of the (physical) oscillator mode $\lambda$. An extensive but elementary calculation [] reveals that $\tilde{\rho} = |0_{AB}\rangle\langle 0_{AB}|$ with $|0_{AB}\rangle = |0_A\rangle \otimes |0_B\rangle$ satisfies Eq. (2.42). The doubling in degrees of freedom ensures that the reduced density matrix obtained from an initial pure state $|\tilde{\Psi}_0\rangle = |\psi_0\rangle \otimes |0_{AB}\rangle$ in the enlarged Hilbert space coincides with the original state at finite temperature (2.40). Expressed in these new coordinates the total Hamiltonian (2.41) reads

$$
\begin{aligned}
H_{\mathrm{tot}} = H \otimes \mathrm{I} &+ \sum_\lambda \sqrt{\bar{n}_\lambda + 1} \left( g_\lambda^* L \otimes A_\lambda^\dagger + g_\lambda L^\dagger \otimes A_\lambda \right) \\
&+ \sum_\lambda \sqrt{\bar{n}_\lambda} \left( g_\lambda L^\dagger \otimes B_\lambda^\dagger + g_\lambda^* L \otimes B_\lambda \right) \\
&+ \mathrm{I} \otimes \sum_\lambda \omega_\lambda \left( A_\lambda^\dagger A_\lambda - B_\lambda^\dagger B_\lambda \right).
\end{aligned}
\tag{2.43}
$$

This is identical to the zero-temperature model, except now the system is couples to two separate oscillator baths instead of one. Therefore, we need two independent processes $Z_t^*$ and $W_t^*$ for a stochastic version of Eq. (2.43) in general:

$$
\begin{aligned}
\partial_t \psi_t = -\mathrm{i} H \psi_t &+ L Z_t^* \psi_t - L^\dagger \int_0^t \alpha_1(t-s) \frac{\delta\psi_t}{\delta Z_s^*}\, \mathrm{d}s \\
&+ L^\dagger W_t^* \psi_t - L \int_0^t \alpha_2(t-s) \frac{\delta\psi_t}{\delta W_s^*}\, \mathrm{d}s.
\end{aligned}
\tag{2.44}
$$

All effects of the original thermal initial state are now encoded in the correlation functions

$$\alpha_1(t) = \sum_\lambda (\bar{n}_\lambda + 1)|g_\lambda|^2 \mathrm{e}^{-\mathrm{i}\omega_\lambda t} \quad \text{and} \quad \alpha_2(t) = \sum_\lambda \bar{n}_\lambda |g_\lambda|^2 \mathrm{e}^{\mathrm{i}\omega_\lambda t} \tag{2.45}$$

for $Z_t^*$ and $W_t^*$ respectively. Both are Gaussian, thus independence of $Z^*$ and $W^*$ is equivalent to vanishing mutual covariance $\mathbb{E}\left(Z_t^* W_s\right) = \mathbb{E}\left(Z_t W_s\right) = 0$.

As we doubled the bath degrees of freedom merely to cope with a thermal initial state, it is quite natural that the zero-temperature result (2.13) with a single noise process is recovered in the limit $T \to 0$: With vanishing occupation numbers $n_\lambda \to 0$ both, $\alpha_2$ and $W_t^*$, go to zero, while $\alpha_1$ reproduces the original bath correlation function (2.7).

The thermo-field approach is especially simple for a self-adjoint coupling operator $L = L^\dagger$. Indeed, we can combine both processes in Eq. (2.44) into a single one, which we denote by $\tilde{Z}_t^*$. Since $Z^*$ and $W^*$ are mutual independent by assumption and $2\bar{n}_\lambda + 1 = \coth \frac{\beta\omega_\lambda}{2}$, we find for the crucial correlation function

$$\mathbb{E}\left(\tilde{Z}_t \tilde{Z}_s^*\right) = \sum_\lambda \left( |g_\lambda|^2 \coth \frac{\beta\omega_\lambda}{2} \cos\omega_\lambda(t-s) - \mathrm{i}\sin\omega_\lambda(t-s) \right). \qquad (2.46)$$

Consequently, the finite temperature NMSSE with self-adjoint coupling operators is identical to the $T = 0$ result except for a modified correlation function. It is not surprising that the combined correlation function (2.46) agrees with the result of Feynman and Vernon already encountered in Eq. (2.6), which is usually derived by means of path integration [14]. But the approach presented here is much more general since it can tackle any kind of open quantum system with linear coupling.

## 2.6. Jaynes-Cummings Model

The Jaynes-Cummings model was originally introduced to study the decay of an atom coupled to a single quantized mode of the electro-magnetic field in a cavity [25]. It describes a single electronic excitation of the atom with energy $\omega$ above ground state in terms of an effective two level system with $H = \frac{\omega}{2}\sigma_z$. Other electronic levels can be neglected safely, if their excitation energy is much larger than $\omega$ or far off-resonance compared to the cavity mode. We approximate the coupling operator to the cavity-mode within dipole and rotating-wave approximation as $L = g\sigma_-$. This approximation holds as long as the coupling strength $g$ is very small compared to the cavity transition frequency. Only recently, experiments in circuit quantum electrodynamics detected effects from so called counter-rotating interaction terms [32].

In summary, the NMSSE for the Jaynes-Cummings model at zero temperature reads

$$\partial_t \psi_t = -\mathrm{i}\frac{\omega}{2}\sigma_z\psi_t + g\sigma_- Z_t^* \psi_t - g\sigma_+ \int_0^t \alpha(t-s)\frac{\delta\psi_t}{\delta Z_s^*}\,\mathrm{d}s. \qquad (2.47)$$

This also covers the more general case of a possibly structured environment.

### 2.6.1. O-Operator Method

As elaborated in Sect. 2.2.1 we can simplify the NMSSE (2.47) by replacing the functional derivative with an operator $O(t, s, Z^*)$. We try to solve the consistency condition (2.18) by a noise-independent ansatz

$$O(t, s) = gf(t, s)\sigma_-. \qquad (2.48)$$

Hence, all non-Markovian feedback from the environment is now encoded in the function $f(t, s)$ to be determined. Plugging this ansatz into the evolution equation for $O$ yields

$$\partial_t f(t, s)\sigma_- = \left[-\mathrm{i}\frac{\omega}{2}\sigma_z - g^2 F(t)\sigma_+\sigma_-, f(t, s)\sigma_-\right] \qquad (2.49)$$

with a shorthand notation $F(t) := \int_0^t \alpha(t-s)f(t, s)\,\mathrm{d}s$. From its definition (2.17) we see that $F$ is also the coefficient of the integrated operator $\bar{O}(t) = gF(t)\sigma_-$. Since the operator algebra in Eq. (2.49) closes, our ansatz solves the equation of motion for $O$ provided $f$ evolves according to

$$\partial_t f(t, s) = \left(\mathrm{i}\omega + g^2 F(t)\right) f(t, s), \qquad 0 \le s \le t.$$

Appropriate initial conditions follow trivially from Eq. (2.19), namely $f(s, s) = 1$. In the special case of an exponential bath correlation function $\alpha(t) = \mathrm{e}^{-\gamma|t| - \mathrm{i}\Omega t}$ we can also derive a differential equation that is closed in $F$, namely

$$\partial_t F(t) = 1 + (\mathrm{i}(\omega - \Omega) - \gamma)F(t) + g^2 F(t)^2. \qquad (2.50)$$

Such exponential correlation functions $\alpha(t) = \mathrm{e}^{-\gamma|t| - \mathrm{i}\Omega t}$ play a major role in the subsequent work. Once $F$ is known we can determine solutions of the convolutionless NMSSE for given noise realizations or—since $O$ is independent of $Z^*$—directly calculate the reduced density operator using a master equation similar to Eq. (2.27).

### 2.6.2. Noise-Expansion Method

In this section we propose a different approach to Eq. (2.47): It is based on the expansion discussed in Sect. 2.4, which allows us to express the quantum trajectories $\psi_t(Z^*)$ in a functional Taylor series with respect to the noise process

$$\psi_t(Z^*) = \begin{pmatrix} \psi^+(t) \\ \psi^-(t) \end{pmatrix} + \int_0^t \begin{pmatrix} \psi_s^+(t) \\ \psi_s^-(t) \end{pmatrix} Z_s^* \, \mathrm{d}s.$$

Due to the particular coupling structure of the model we can neglect all terms higher than linear order in $Z_t^*$. As further elaborated in Sect. A.1 our NMSSE (2.47) reduces to a $\mathbb{C}$-valued integro-differential equation

$$\dot{\psi}^+(t) = -\mathrm{i}\frac{\omega}{2}\psi^+(t) - g^2 \int_0^t \alpha(t-s)\mathrm{e}^{\mathrm{i}\frac{\omega}{2}(t-s)}\psi^+(s) \, \mathrm{d}s, \qquad (2.51)$$

which is nevertheless quite involved—even from a numerical point of view. Again, the situation simplifies dramatically for an exponential correlation function; the details are provided in Sect. A.1 as well.

Nevertheless, we may still discover some illuminating consequences concerning the $O$-operator without an explicit solution for $\psi^+(t)$. With $\psi^-(t) = \psi^-(0)\exp(\mathrm{i}\omega t/2)$ the full quantum trajectory reads

$$\psi_t(Z^*) = \begin{pmatrix} \psi^+(t) \\ \psi^-(t) \end{pmatrix} + g \int_0^t \begin{pmatrix} 0 \\ \mathrm{e}^{\mathrm{i}\frac{\omega}{2}(t-s)}\psi^+(s) \end{pmatrix} Z_s^* \, \mathrm{d}s. \qquad (2.52)$$

This allows us to calculate the functional derivative with respect to the noise process explicitly; for $0 < s < t$ we find

$$\frac{\delta\psi_t(Z^*)}{\delta Z_s^*} = g \begin{pmatrix} 0 \\ \mathrm{e}^{\mathrm{i}\frac{\omega}{2}(t-s)}\psi^+(s) \end{pmatrix},$$

which agrees with our ansatz (2.48) if we choose

$$f(t,s) = \frac{\psi^+(s)}{\psi^+(t)}\,\mathrm{e}^{\mathrm{i}\frac{\omega}{2}(t-s)}. \qquad (2.53)$$

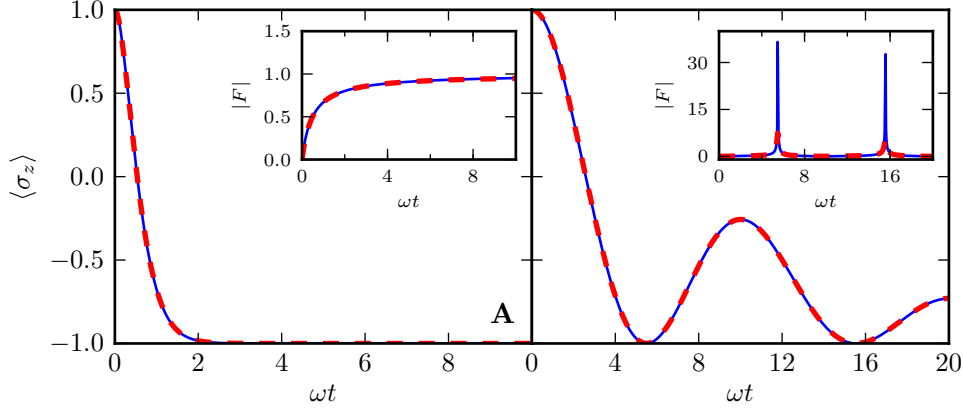A similar structure for the $O$-operator has been obtained before using a Heisenberg-

**Figure 2.2.:** Jaynes-Cummings model with an exponentially decaying bath correlation function $\alpha(t) = \frac{\gamma}{2}e^{-\gamma|t|-i\Omega t}$ in resonance ($\Omega = \omega$) and coupling strength $g = \sqrt{2}$ calculated using Eq. (A.11). Insets show $|F|$ representing magnitude of $\bar{O}$. **(A)** Strongly damped $\gamma = 4\omega$, **(B)** Weakly damped $\gamma = 0.1\omega$; the dashed line represent the same parameter set, but slightly moved off-resonance ($\Omega = 1.01\omega$).

operator technique [47].

Recall that the convolutionless NMSSE of the last section reduces to a nonlinear differential equation (2.50) for

$$F(t) = \int_0^t \alpha(t-s)e^{i\frac{\omega}{2}(t-s)}\frac{\psi^+(s)}{\psi^+(t)}\,ds, \tag{2.54}$$

where $f(t,s)$ has already been replaced by the expression (2.53), derived using the noise expansion. We will now argue that it is exactly the denominator $\psi^+(t)$ that may cause problems in a numerical integration of (2.50): Indeed, calculating the reduced density matrix from Eq. (2.52) and using the condition $\operatorname{Tr}\rho_t = 1$, we find the connection $\langle\sigma_z\rangle_{\rho_t} = 2|\psi^+(t)|^2 - 1$.

Since for $\gamma \neq 0$ the Jaynes-Cummings model is expected to relax to the electronic ground state, namely the eigenstate of $\sigma_z$ with eigenvalue $-1$, the denominator in (2.54) eventually goes to zero. Even worse are local extremal points $t_i$, where $\langle\sigma_z\rangle_{\rho_t} \approx -1$, as we see in Fig. 2.2: The excitation in A decays almost exponentially due to the small memory time $\tau = \gamma^{-1}$ of the environment. Therefore, $\frac{\psi^+(s)}{\psi^+(t)} \approx 1$ in

the relevant time scale $s \in [t - \tau, t]$ of Eq. (2.54), so $|F|$ approaches a constant value uniformly. In contrast, the highly non-Markovian system B shows singular peaks in $|F|$ for $\omega t \approx 5, 15$, where the expectation value of $\sigma_z$ is approximately $-1$. These result from large fractions $\frac{\psi^+(s)}{\psi^+(t)}$, as the correlation function $\alpha$ does not decay rapidly enough to suppress contributions in the integral with $\psi^+(s) \gg \psi^+(t)$.

This resonant behavior is not surprising since deriving Eq. (2.50) once with respect to time yields a differential equation related to the dynamical equation of a damped harmonic oscillator. Also, notice how shifting the bath-frequency $\Omega$ only slightly off-resonance results in a much smoother $F$—as the dashed line in Fig. 2.2 B shows—while $\langle \sigma_z \rangle$ remains virtually unchanged. Actually, these large peaks do not contribute excessively to the end result, as they are canceled with the very small value of $\psi^+(t)$ in $\bar{O}(t)\psi_t(Z^*)$ (or in the corresponding master equation). Still, the numerical solution of Eq. (2.50) requires a more careful treatment for the resonant case in order to correctly reproduce these peaks and not diverge to infinity.

Of course all statements made in this section only hold for the simple Jaynes-Cummings model, and it is not clear, whether the $\bar{O}$-operator behaves similarly for more realistic systems. Notwithstanding, an even more problematic behavior of $\max_{m,n} |\bar{O}_{mn}(t)|$, where $\bar{O}_{mn}(t)$ are the matrix elements of $\bar{O}(t)$ in the system-basis used, has been found in ZOFE[7] and the related higher-order calculation for certain parameter regimes of more realistic systems. As for a larger number of bath modes resonances are more likely to occur, the situation is much more delicate for them. Likely, these numerical sophisticated problems are also responsible for divergences of higher order hierarchies in the $O$-operator making a systematic improvement of ZOFE quite involved. We come to the conclusion that it can be advantageous to devise a numerical scheme in terms of the more regular $\bar{O}(t, Z^*)\psi_t(Z^*)$ instead, as sharp contributions during the propagation might be smoothed away—this is exactly the approach used for our stochastic hierarchical equations of motion presented in the next chapter.

---

[7]Gerhard Ritschel, private communications. The zero-order functional expansion (ZOFE) was introduced in Sect. 1.3.

# 3. Numerical treatment

The Jaynes-Cummings model from the end of the last chapter is one of the rare cases where an analytical ansatz for $\bar{O}$ is known. Numerical solution-methods of the convolutionless non-Markovian stochastic Schrödinger equation usually attack the consistency condition (2.18) directly using an expansion with respect to the noise. Although this provides a very efficient algorithm for large parameter regimes, a systematic improvement of accuracy seems intractable [].

With recent advances in super-computing, realistic biological and chemical systems came within the reach of the far more costly, but better-behaved and formally exact hierarchical-equations-of-motion (HEOM) approach []. Although formally equivalent to the Feynman-Vernon influence functional, the HEOM-formalism is much better suited for numerical investigation, since it provides a systematic way to check convergence and does not require evaluation of highly-oscillatory path integrals. Summarized shortly, it amounts to dealing with memory effects in the influence-functional by introducing additional auxiliary density matrices (ADM). However, the number of ADMs grows rapidly for highly non-Markovian systems. Combined with the $N^2$-scaling of the memory requirement[1] with the system's dimension $N$, this places enormous demands on the computational infrastructure.

The last point emphasizes why stochastic unravellings are often preferred over the corresponding master equation for very large Markovian systems: Memory-demand from pure states scales linearly with the size of the system and even the propagation matrices grow at most quadratically. Just as essential for modern supercomputers is the ability to run individual realizations completely independent, allowing highly efficient parallelization to many thousand cores.

It this chapter we present the main result of this work: a hierarchy of stochastic,

---

[1]Sparse.matrix algorithms are able to reduce the $N^4$-scaling of the propagation matrices, but still, these are even more problematic than the ADMs.

pure state trajectories in the spirit of the established density matrix hierarchy. For that matter we outline the HEOM-formalism in Sect. 3.1. Afterwards, we derive the pure state hierarchy based on the NMSSE in its linear, as well as nonlinear version. As a closed set of equations crucially relies on an exponential bath correlation function (or sums thereof), Sect. 3.3 is devoted to an expansion of more general spectral densities at finite temperature leading to the sought-after form. Finally, we apply the hierarchy of stochastic pure states to the Spin-Boson model, investigating its accuracy in dependence on the sample size and number of auxiliary states.

## 3.1. Hierarchical Equations of Motion

SHORT OUTLINE

## 3.2. Stochastic Hierarchical Equations of Motion

In this section we present the main results of this work, namely an approach to solve the non-Markovian stochastic Schrödinger equation

$$\partial \psi_t = -\mathrm{i}h\psi_t + LZ_t^*\psi_t - L^\dagger \int_0^t \alpha(t-s)\frac{\delta \psi_t}{\delta Z_s^*}\,\mathrm{d}s \tag{3.1}$$

numerically without resorting to the $O$-operator substitution. Therefore, we need to conceive a different way to deal with the non-locality of the functional derivative with respect to time and process realization, as it prevents the application of efficient Monte-Carlo methods, which are used to deal with stochastic Schrödinger equations in the Markovian regime [8,35].

It turns out that for certain correlation functions the linear NMSSE (3.1) is formally equivalent to an infinite hierarchy of completely local stochastic differential equations. Although we borrow the main idea from the hierarchical equations of motion presented in the previous section, we need to deal with some peculiarities of our NMSSE, first.

### 3.2.1. Linear Hierarchy

The basic idea is to absorb the action of the functional derivative on $\psi_t(Z^*)$ into an auxiliary pure state

$$\psi_t^{(1)}(Z^*) := \int_0^t \alpha(t-s)\frac{\delta\psi_t(Z^*)}{\delta Z_s^*}\,\mathrm{d}s. \qquad (3.2)$$

Hereinafter, we use the term "state" quite loosely for any vector in the system's Hilbert space regardless of its norm. Recall that the integral boundaries arise only after we apply the derivative on states $\psi_t(Z^*)$ that satisfy the additional condition $\delta\psi_t(Z^*)/\delta Z_s^* = 0$ for $s < 0$ and $s > t$. Therefore, we may write Eq. (3.2) more concisely as

$$\psi_t^{(1)}(Z^*) = \left(\int \alpha(t-s)\frac{\delta}{\delta Z_s^*}\,\mathrm{d}s\right)\psi_t(Z^*) =: \mathcal{D}_t\psi_t(Z^*)$$

with the integrated functional derivation operator $\mathcal{D}_t$. For a finite environment, $\mathcal{D}_t$ is simply the adjoint of the force operator (2.5).

The equation of motion for $\psi_t^{(1)}(Z^*)$ takes a form similar to the original NMSSE (3.1), provided $\dot{\mathcal{D}}_t = \int \dot{\alpha}(t-s)\,\delta/\delta Z_s^*\,\mathrm{d}s$ can be expressed in terms of known quantities. Of course, the simplest choice is an exponential bath correlation function

$$\alpha(t) = g\,\mathrm{e}^{-\gamma|t|-\mathrm{i}\Omega t}. \qquad (3.3)$$

with $g$, $\gamma$ and $\Omega$ real. The absolute value of $t$ in the exponent is necessary to ensure hermiticity $\alpha(-t) = \alpha(t)^*$. In Sect. B.1 we elaborate that such a correlation function simply gives

$$\dot{\mathcal{D}}_t\psi_t(Z^*) = -(\gamma+\mathrm{i}\Omega)\mathcal{D}_t\psi_t(Z^*) \qquad (3.4)$$

for solutions $\psi_t(Z^*)$ of the NMSSE with vacuum initial conditions. We abbreviate the coefficient $w = \gamma + \mathrm{i}\Omega$ in order to simplify notation.

Now, let use return to the NMSSE; with the auxiliary stochastic state (3.2) it can be expressed as an inhomogeneous stochastic equation, namely

$$\partial_t\psi_t(Z^*) = -\mathrm{i}H\psi_t(Z^*) + LZ_t^*\psi_t(Z^*) - L^\dagger\psi_t^{(1)}(Z^*).$$

By the construction in the previous paragraph the last term satisfies a closely related

equation:

$$\partial_t(\mathcal{D}_t\psi_t) = -w\mathcal{D}_t\psi_t + \mathcal{D}_t(-\mathrm{i}H + LZ_t^* - L^\dagger\mathcal{D}_t)\psi_t$$
$$= (-\mathrm{i}H - w + LZ_t^*)\psi_t^{(1)} + [\mathcal{D}_t, Z_t^*]L\psi_t - L^\dagger\mathcal{D}_t\psi_t^{(1)}. \tag{3.5}$$

Naturally, $\mathcal{D}_t$ commutes with all system operators and itself. It is not surprising that the functional derivative reappears in the equation for $\psi_t^{(1)}$; therefore, we need to introduce another auxiliary state $\psi_t^{(2)}(Z^*)$. This scheme leads to an infinite hierarchy of stochastic vectors in the system's Hilbert space

$$\psi_t^{(k)}(Z^*) := \mathcal{D}_t\psi_t^{(k-1)}(Z^*) = \mathcal{D}_t^k\psi_t(Z^*). \tag{3.6}$$

Expressed in the new auxiliary states and with $[\mathcal{D}_t, Z_s^*] = \alpha(t-s)$, Eq. (3.5) reads

$$\partial_t\psi_t^{(1)} = (-\mathrm{i}H - w + LZ_t^*)\psi_t^{(1)} + \alpha(0)L\psi_t^{(0)} - L^\dagger\psi_t^{(2)}.$$

Along these lines it is straightforward to derive the full hierarchy of equations of motions for all $\psi_t^{(k)}$. Since the commutator $[\mathcal{D}_t, Z_s^*]$ is a $\mathbb{C}$-number, each auxiliary state only couples to the order directly above and below

$$\partial_t\psi_t^{(k)} = (-\mathrm{i}H - kw + LZ_t^*)\psi_t^{(k)} + k\alpha(0)\psi_t^{(k-1)} - L^\dagger\psi_t^{(k+1)}. \tag{3.7}$$

The vacuum initial condition for the true quantum trajectory $\delta\psi_0/\delta Z_s^* = 0$ requires all auxiliary states to vanish at $t = 0$.

Of course the infinite hierarchy is even more intricate to solve than the original NMSSE . To transform  Eq. (3.7) into a practical scheme, we truncate the hierarchy at finite order.  It is quite remarkable that this can be done in a self-consistent manner, which even incorporates the neglected orders approximately. This is derived most clearly using the equivalent integral equation for $\psi_t^{(k)}$

$$\psi_t^{(k)} = \int_0^t e^{-kw(t-s)}\, \mathrm{T}_+ e^{\int_s^t -\mathrm{i}H + LZ_u^*\,\mathrm{d}u} \left(k\alpha(0)L\psi_s^{(k-1)} - L^\dagger\psi_s^{(k+1)}\right)\,\mathrm{d}s, \tag{3.8}$$

as it satisfies  Eq. (3.7) and the correct initial conditions. For $k$ large enough, the first exponential is approximately zero once $s \neq t$, thus the remaining integrand only gives

a contribution for $s = t$ and can be safely extracted from the integral[2]. Evaluating the rest of the integral simply gives $\frac{1 - \exp(-kwt)}{kw}$. As the second summand is relevant only for very small times $t$, it is dropped in the following work—including it in a numerical implementation is straightforward. Thus, we have an approximate expression for the $k^{\text{th}}$-order auxiliary state

$$\psi_t^{(k)} = \frac{\alpha(0)}{w} L \psi_t^{(k-1)} - \frac{1}{kw} L^\dagger \psi_t^{(k+1)}. \tag{3.9}$$

If we further assume that the second term, coupling to the order above, is suppressed by the prefactor $\frac{1}{kw}$, the infinite hierarchy terminates at finite order. The remainder of Eq. (3.9), namely

$$\psi_t^{(k)} = \frac{\alpha(0)}{w} L \psi_t^{(k-1)}, \tag{3.10}$$

is called "terminator" of the hierarchy. For $w = \gamma$, this procedure can be interpreted as a Markov approximation for the $(k-1)^{\text{th}}$ auxiliary state similar to Eq. (2.23), although the driving process is not affected at all.

### 3.2.2. Nonlinear Hierarchy

We mentioned in Sect. 2.3 how the scaling with sampling size of our Monte-Carlo scheme improves greatly, if we use comoving environmental basis states (2.36) and the corresponding nonlinear NMSSE . Up to a certain extend this idea can also be applied to our hierarchical equations of motion.

Seen as a function of coherent state labels $\boldsymbol{z}^*$ instead of the process $Z^*$, the Girsanov-transformed auxiliary states are defined by

$$\tilde{\psi}_t^{(k)}(\boldsymbol{z}^*) := (\psi_t^{(k)} \circ \boldsymbol{\phi}_t)(\boldsymbol{z}^*) = \psi_t^{(k)}(\boldsymbol{\phi}_t(\boldsymbol{z}^*))$$

using the "phase-space" flow (2.36). Then, along the lines of the derivation leading to Eq. (3.7) we obtain its nonlinear form

$$\partial_t \tilde{\psi}_t^{(k)}(\boldsymbol{z}^*) = \left( -iH - kw + LZ_t^* + L \int_0^t \alpha(t-s)^* \langle L^\dagger \rangle_s \, ds \right) \tilde{\psi}_t^{(k)}(\boldsymbol{z}^*)$$
$$+ k\alpha(0) L \tilde{\psi}_t^{(k-1)} - (L^\dagger - \langle L^\dagger \rangle_t) \tilde{\psi}_t^{(k+1)}(\boldsymbol{z}^*), \tag{3.11}$$

---

[2]We postpone the more formal discussion to Sect. B.2.

with the normalized expectation value taken with respect to the true quantum trajectory—or, put differently, with respect to the zeroth order auxiliary state

$$\langle L^\dagger \rangle_t = \frac{\langle \tilde{\psi}_t^{(0)} | L^\dagger | \tilde{\psi}_t^{(0)} \rangle}{\langle \tilde{\psi}_t^{(0)} | \tilde{\psi}_t^{(0)} \rangle}. \tag{3.12}$$

Deriving a terminator for the nonlinear version is completely analog to Eq. (3.10) and gives the same result.

Notice that the exponential correlation function necessary for the hierarchy also simplifies the treatment of the memory-term in Eq. (3.11). Indeed $f(t) := \int_0^t \alpha(t-s)^* \langle L^\dagger \rangle_s \, \mathrm{d}s$ satisfies

$$\dot{f}(t) = \alpha(0) \langle L^\dagger \rangle_t - w^* f(t) \tag{3.13}$$

Therefore, we only need to store the hierarchy and auxiliary function $f$ for one time step in a numerical implementation—making this approach very memory-efficient.

But one caveat remains: for the convolutionless formulation we can go one step further and derive an equation for normalized pure state trajectories (2.39). However, such a hierarchy with all auxiliary states having unit norm seems to be unobtainable. Nonetheless, we hope that there is another version of the nonlinear hierarchy, which achieves a normalized zero-order state—this would tremendously improve the numerical accuracy of the expectation values (3.12) for large $\langle \tilde{\psi}_t^{(0)} | \tilde{\psi}_t^{(0)} \rangle$, as it occurs for very strong coupling[3].

### 3.2.3. Multiple Modes

Of course, most interesting systems cannot be modeled using a single exponential decaying correlation function (3.3). To accommodate a more complex environmental structure, we modify the hierarchy to handle a finite number of exponential modes coupling to the system with arbitrary operators. As the crucial points do not depend on the choice of linear or nonlinear version, we are only concerned with the former in this section to simplify notation.

The linear NMSSE for a finite number $N$ of independent environments is derived

---

[3]I would like to thank Richard Hartmann for pointing this out.

similarly to the lines of Sect. 2.2 and reads

$$\partial_t \psi_t = -\mathrm{i}H\psi_t + \sum_{j=1}^{N} L_j Z_{j,t}^* \psi_t - \sum_{j=1}^{N} L_j^\dagger \int_0^t \alpha_j(t-s) \frac{\delta \psi_t}{\delta Z_{j,t}^*} \, \mathrm{d}s \qquad (3.14)$$

with mutually independent noise processes satisfying

$$\mathbb{E}\, Z_{i,t} = 0, \quad \mathbb{E}\, Z_{i,t} Z_{j,s} = 0, \quad \text{and} \quad \mathbb{E}\, Z_{i,t} Z_{j,s}^* = \delta_{ij} \alpha_i(t-s).$$

Just as in the single-mode case, Eq. (3.14) is equivalent to an infinite hierarchy of auxiliary states if all correlation functions take the exponential form (3.3). Since all derivation operators $\mathcal{D}_{j,t}$ corresponding to the processes $Z_{j,t}^*$ mutually commute, the most general form of an auxiliary state is given by

$$\psi_t^{(k_1,\ldots,k_N)} := \mathcal{D}_{1,t}^{k_1} \ldots \mathcal{D}_{N,t}^{k_N} \psi_t. \qquad (3.15)$$

Hereinafter, we use boldface symbols to abbreviate $N$-tuples such as $\boldsymbol{k} = (k_1,\ldots,k_n)$. Summarily, the infinite hierarchy appertaining to Eq. (3.14) reads

$$\partial_t \psi_t^{(\boldsymbol{k})} = \left( -\mathrm{i}H - \boldsymbol{k} \cdot \boldsymbol{w} + \sum_j L_j Z_{j,t}^* \right) \psi_t^{(\boldsymbol{k})} + \sum_j k_j \alpha_j(0) \psi_t^{(\boldsymbol{k}-\boldsymbol{e}_j)} - \sum_j L_j^\dagger \psi_t^{(\boldsymbol{k}+\boldsymbol{e}_j)}, \qquad (3.16)$$

where $\boldsymbol{e}_j$ denotes the $j$-th unit vector in $\mathbb{R}^N$ and $\boldsymbol{k} \cdot \boldsymbol{w} = \sum_j k_j w_j$ is the euclidean scalar product[4].

When it comes to truncating the hierarchy (3.16) the most obvious strategy is simply to cut off each mode separately at given order $D$. In other words the truncation condition reads $0 \le k_j \le D$ for all $j = 1,\ldots,N$; any auxiliary state not satisfying it is either set to zero or replaced by the terminator

$$\psi^{(\boldsymbol{k}+\boldsymbol{e}_j)} = \sum_i \frac{(\boldsymbol{k}+\boldsymbol{e}_j)_i \, \alpha_i(0)}{(\boldsymbol{k}+\boldsymbol{e}_j) \cdot \boldsymbol{w}} L_i \psi_t^{(\boldsymbol{k}+\boldsymbol{e}_j-\boldsymbol{e}_i)}.$$

We refer to this as the "cubic truncation scheme" since the hierarchy's shape resembles

---

[4] Although $\boldsymbol{w}$ is complex in general, the scalar product $\boldsymbol{k} \cdot \boldsymbol{w}$ does not involve complex conjugation.
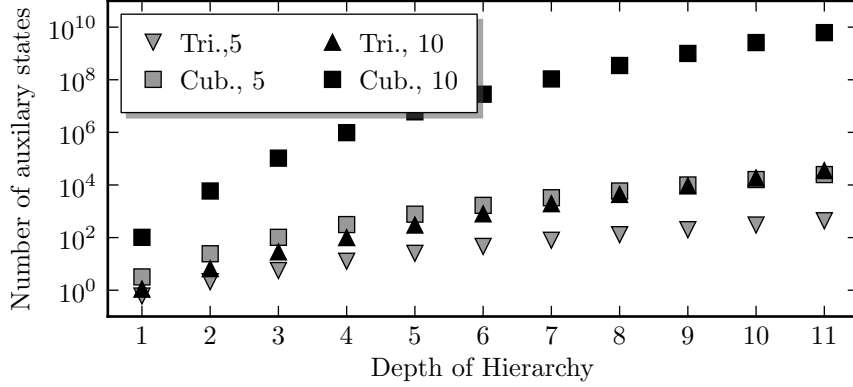
**Figure 3.1.:** Scaling of the number of auxiliary states with the truncation order $D$ and number of modes $N$. Even for relatively small $N$ the triangular scheme (3.17) is far superior compared to the cubic truncation scheme with an exponential scaling law $(D+1)^N$.

an $N$-cube. Clearly, the number of auxiliary states scales exponentially like $(D+1)^N$, which makes the treatment of large systems with a highly structured spectral density virtually impossible.

Examining Eq. (3.16) closer, we notice that the term responsible for suppression of the $\boldsymbol{k}^{\text{th}}$ auxiliary state is $\exp(-\boldsymbol{k}\cdot\boldsymbol{w})$. Instead of treating each mode individually, we use a condition better suited for the product $\boldsymbol{k}\cdot\boldsymbol{w}$, namely $0\leq|\boldsymbol{k}|\leq D$ with $|\boldsymbol{k}|=\sum_j k_j$. For $N=2$ the corresponding states form a triangular shape—hence the name "triangular truncation scheme". The appropriate generalization to an arbitrary number of modes is an $N$-simplex with the number of elements given by

$$\sum_{d=0}^{D}\binom{d+N-1}{N-1}=\frac{(D+N)!}{D!N!},\tag{3.17}$$

showing a much softer scaling with $N$ compared to the cubic scheme. In Fig. 3.1 we display the number of auxiliary states required for a given number of modes and truncation order $D$. Clearly, the triangular truncation is far superior although for small $N$ both methods are applicable. The difference is more pronounced for larger $N$ required in the study of realistic systems.

Depending on the specific problem, additional truncation conditions may reduce the computational expenses without sacrificing accuracy. Especially environments that mix modes with large memory times and almost-Markovian modes provide many

options for optimization. However, we do not elaborate this point any further and rely on the triangular truncation throughout this work.

## 3.3. Correlation Function Expansion

Applicability of our hierarchical equations of motion to certain model depends predominantly on the ability to express the relevant bath correlation function

$$\alpha(t-s) = \int_0^\infty J(\omega) \left( \coth\left( \frac{\beta\omega}{2} \right) \cos\omega(t-s) - \mathrm{i}\sin\omega(t-s) \right) \mathrm{d}\omega \qquad (3.18)$$

as a sum of exponentials like (3.3). Such exponentials arise as Fourier transforms of a Lorentzian spectral density

$$J(\omega) = \frac{1}{\pi} \frac{\gamma}{(\omega - \Omega)^2 + \gamma^2}. \qquad (3.19)$$

Hence they can be obtained from Eq. (3.18) in the zero-temperature limit provided we extend the integral domain to include arbitrary negative frequencies as well. This unphysical assumption seems to be a good approximation to the exact case without negative frequencies for certain parameters as Fig. 3.2 shows: For $\gamma \ll \Omega$ the Lorentzian density $J$ is concentrated on the positive semi-axis and the negative frequency contributions vanish primarily. However, Eq. (3.19) is a prime example of a heavy-tailed distribution, having no finite moments except $\int J(\omega)\,\mathrm{d}\omega = 1$, so this approximation needs to be handled with care.

A more systematic way to obtain the desired bath correlation function in the case $T > 0$ involves anti-symmetrized spectral densities $\tilde{J}(\omega) := J(\omega) - J(-\omega)$. This way, negative frequencies are included without any approximation. Indeed, since $\tilde{J}$, coth, and sin are anti-symmetric and cos is symmetric with respect to reflection at the origin we have

$$\int_0^\infty \tilde{J}(\omega)(\dots)\mathrm{d}\omega = \frac{1}{2} \int_{-\infty}^\infty \tilde{J}(\omega)(\dots)\mathrm{d}\omega. \qquad (3.20)$$

Commonly used examples are Drude spectral densities in the HEOM-formalism (see Sect. B.3) or sums of anti-symmetrized Lorentzians, which are well suited to approximate highly-structured environments [31]. Although the discussion below works for
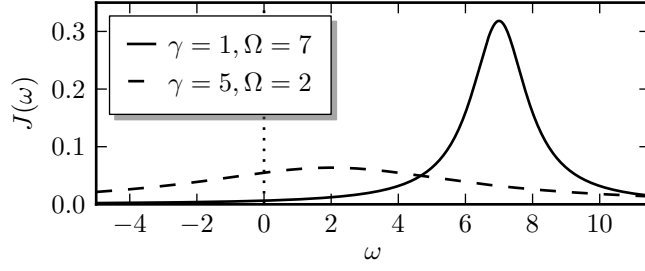
**Figure 3.2.:** Schematic comparison of Lorentzian spectral densities used to obtain exponential bath correlation functions (see Eq. (3.19) for notation). For $\gamma \ll \Omega$ (blue line) the weight is concentrated on the positive semi-axis.

a much larger class of spectral densities [37], we assume $\tilde{J}$ to have a finite number of mutually distinct poles lying off the real and imaginary axis like $\tilde{J}$ obtained from Eq. (3.19).

To calculate the correlation function, we evaluate the integral (3.20) analytically using the residue theorem. While the poles of the anti-symmetric spectral density $\tilde{J}$ are assumed to be known, there are different expansion schemes for the hyperbolic cotangens: Since many established HEOM-results are based on the Matsubara-spectrum decomposition, it is presented in detail. Nevertheless, it has been brought forward only recently that the Padé-expansion provides superior approximation scheme, especially for low temperature [21, 22]. We achieve a much more convenient form by treating the real- and imaginary part of $\alpha(t) = a(t) + ib(t)$ separately, where the former

$$a(t) = \frac{1}{2} \int_{-\infty}^{\infty} \tilde{J}(\omega) \coth\left(\frac{\beta\omega}{2}\right) \cos\omega t \, \mathrm{d}\omega = \frac{1}{2} \int_{-\infty}^{\infty} \tilde{J}(\omega) \coth\left(\frac{\beta\omega}{2}\right) \mathrm{e}^{\mathrm{i}\omega t} \, \mathrm{d}\omega, \quad (3.21)$$

includes all thermal effects, while the imaginary part

$$b(t) = -\frac{1}{2} \int_{-\infty}^{\infty} \tilde{J}(\omega) \sin\omega t \, \mathrm{d}\omega = \frac{1}{2\mathrm{i}} \int_{-\infty}^{\infty} \tilde{J}(\omega) \, \mathrm{e}^{\mathrm{i}\omega t} \, \mathrm{d}\omega$$

is identical for all temperatures.

In order to evaluate Eq. (3.21) for $t > 0$, we close the integration contour in the upper complex half-plane. The poles $\omega = \mathrm{i}\gamma_n = 2\pi\mathrm{i}n/\beta$ of the hyperbolic cotangent

are read off

$$\coth\left(\frac{\beta\omega}{2}\right) = \frac{1 + \mathrm{e}^{-\beta\omega}}{1 - \mathrm{e}^{-\beta\omega}}. \tag{3.22}$$

Indeed, nominator as well as denominator are analytical functions of $\omega$, but the latter vanishes for $\omega = \mathrm{i}\gamma_n$. These are often referred to as Matsubara frequencies. By the usual formula for simple poles, we find for the residuum at the origin

$$\mathrm{Res}_0\left(\coth\frac{\beta\omega}{2}\right) = \lim_{\omega\to 0}\omega\coth\frac{\beta\omega}{2} = \frac{2}{\beta}.$$

Of course, the remaining pole's residua are identical.

Since we assumed that the poles of the spectral density lie off the imaginary axis— or at least are distinct from the poles of the hyperbolic cotangent— Eq. (3.21) for $t > 0$ reduces to a sum over all poles in the upper complex half-plane

$$a(t) = \pi\mathrm{i}\sum_{\omega'}\mathrm{Res}_{\omega'}(\tilde{J})\coth\left(\frac{\beta\omega'}{2}\right)\mathrm{e}^{\mathrm{i}\omega't} + \frac{2\pi\mathrm{i}}{\beta}\sum_{\gamma_n>0}\tilde{J}(\mathrm{i}\gamma_n)\mathrm{e}^{-\gamma_n t}. \tag{3.23}$$

Here, the first sum involves all poles $\omega'$ of $\tilde{J}$ with $\Im\omega' > 0$ and no special care is needed for the coth-pole at $\omega = 0$ since $\tilde{J}(0)$ vanishes anyway. Clearly, $a(t)$ has the desired exponential form; the same hold true for $b(t)$. As $\mathrm{e}^{-\gamma_n t}$ suppresses contributions from large Matsubara frequencies unless $t$ is very small, the infinite sum in Eq. (3.23) is truncated at finite order for numerical purposes.

In conclusion, we obtain an expansion of the bath correlation function of the form

$$\alpha(t) = \sum_n \alpha_n(t) = \sum_n g_n\mathrm{e}^{-w_n t} \qquad (t > 0), \tag{3.24}$$

which is continued to $t < 0$ by $\alpha(-t) = \alpha(t)^*$. But since the prefactors $g_n$ are complex in general, the individual modes $\alpha_n$ do not agree with Eq. (3.3) for negative times. However, this is irrelevant for the derivation of the hierarchy, where $\alpha$ appears merely under the memory integral $\int_0^t \mathrm{d}s\,\alpha(t-s)\ldots$ restricted by vacuum initial conditions. It is only due to the noise processes with correlation $\mathbb{E}Z_{m,t}Z_{n_s}^* = \delta_{mn}\alpha_n(t-s)$, which require $\alpha_m(0) \geq 0$, that we cannot simply apply the result (3.16) to Nevertheless, many spectral densities, for example anti-symmetrized Lorentzians, provide a purely real, positive $\alpha(0)$. This allows us to use a genuine driving process $Z_t^* = \sum_n Z_{n,t}^*$ in

simulations, while building the hierarchy with respect to the expansion (3.24).

## 3.4. Spin-Boson Model

The Spin-Boson model is a paradigmatic model used in the theoretical description of dissipative quantum dynamics [28, 52]. Despite being simple and numerically tractable, it displays properties also found in more complex systems—take for example the transition between a localized, essentially classical phase and a delocalized phase allowing quantum mechanical tunneling [16]. Therefore, it is well suited to investigate properties of dissipative system and the influence of an environment in general. Furthermore, it is often employed as an approximate description of systems with a continuous degree of freedom confined by a double well potential. Examples for the latter are the motion of defects in some crystalline solids or magnetic flux trapped in a superconducting qubit [7]. We use it to demonstrate the superiority of the nonlinear compared to the linear hierarchy as well as the convergence of our hierarchy with increasing depth.

The Spin-Boson model consists of a two-level system with the free time evolution described by the Hamiltonian

$$H = -\frac{1}{2}\Delta\sigma_x + \frac{1}{2}\epsilon\sigma_z,$$

coupled linearly to a bath of harmonic oscillators with $L = \sigma_z$. For simplicity, all calculations in this section involve only a single exponential bath mode with correlation function $\alpha(t) = g\,e^{-\gamma|t|-i\Omega t}$ and real parameters $g$, $\gamma$, $\Omega$.

### 3.4.1. Sample Size

Since our hierarchy is based upon a stochastic differential equation, it is crucial to assess its reliability in dependence on the sample size. In this section we study the convergence of our Monte-Carlo average with respect to the number of realizations. We emphasize in particular the superiority of the nonlinear version (3.11) over the linear hierarchy (3.7). To really emphasize the strengths and weaknesses of both approaches, we choose two quite distinct sets of parameters. Although it is not the only difference between both sets, we refer to them as the weakly and strongly
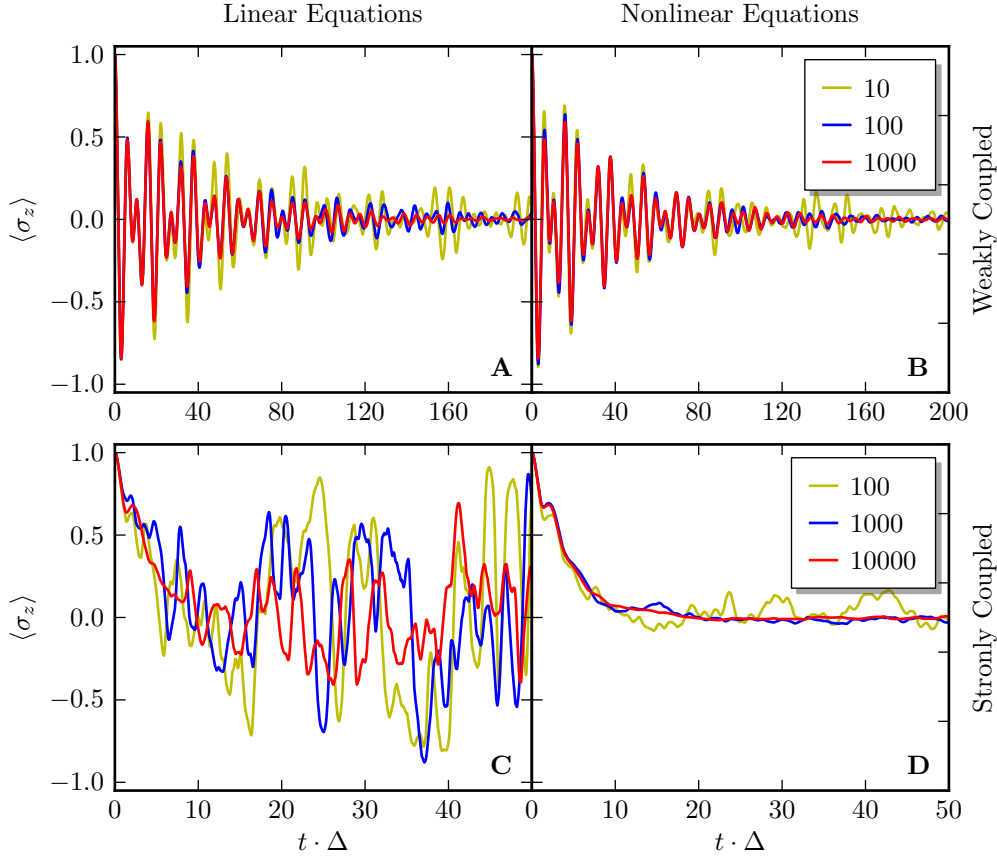
**Figure 3.3.:** $\langle \sigma_z \rangle$ of the symmetric Spin-Boson model ($\epsilon = 0$) using linear(left) and nonlinear(right) stochastic hierarchy. **(A)** and **(C)** weakly coupled system with $g = 0.18\Delta$, $\gamma = 0.05\Delta$ and $\Omega = \Delta$. **(B)** and **(D)** strongly coupled system with $g = 2\Delta$, $\gamma = 0.5\Delta$ and $\Omega = 2\Delta$.
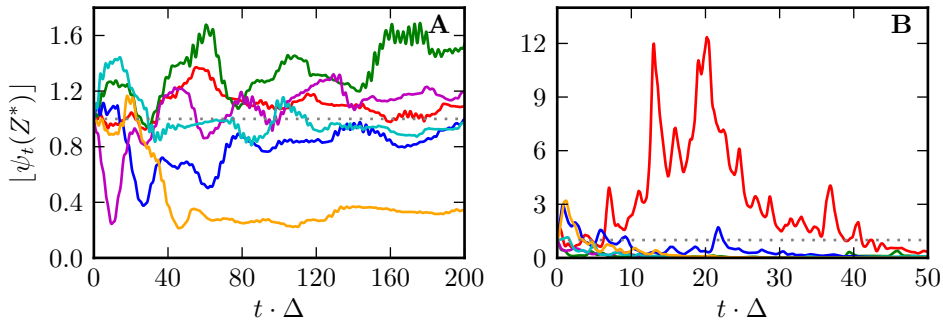


**Figure 3.4.:** Contributions (3.26) of single trajectories to the reduced density operator for the linear equations. **(A)** same parameters as Fig. 3.3 A. **(B)** same parameters as Fig. 3.3 C. The dotted line indicates the contribution of each trajectory for the nonlinear equation.

coupled parameters. The former can even be treated using an improved perturbation scheme [18, 23].

In Fig. 3.3 we plot the expectation value of the spin-operator in $z$-direction for an initial eigenstate "spin up". In the case of weak coupling, shown at the top, there seems to be almost no difference between the linear version on the left and the nonlinear version on the right. Nevertheless, for very few realizations the latter is still in better agreement with the more accurate results. Especially for large times, the dampening on the right hand side is more pronounced as comparing the graph for a sample size of ten reveals.

When it comes to the strongly coupled parameter set at the bottom, the picture changes dramatically: First, notice that the sample size has been increased by an order of magnitude to obtain a reliable result. Notwithstanding the linear version does not display any visible changes for the different sample sizes shown; hence we cannot expect convergence for even larger numbers of realizations. It is only for very small times that both, left and right picture, agree up to a certain extent. In contrast, the nonlinear version improves steadily with growing sample size and already provides a very good approximation with only minor fluctuations at 1000 trajectories. Remarkably, even 100 realizations produce the correct qualitative features as the vanishing of $\langle \sigma_z \rangle$ for large $t$, while the linear hierarchy is not capable of producing equally good results using a sample size more than 100 times larger.

To understand this behavior, recall that we have introduced the nonlinear equations in order to achieve an average over single realizations contributing equal amounts. As already mentioned in Sect. 2.3, individual trajectories of the linear version violate this requirement more or less severely. In order to get a better assessment of different contributions over time we have to rescale the norm as follows: First, we calculate the reduced density operator $\rho_t$ by the usual Monte-Carlo average

$$\rho_t = \sum_{n=1}^{N} |\psi_t(Z_n^*)\rangle\langle\psi_t(Z_n^*)| \tag{3.25}$$

over a large number of noise process realizations $Z_n^*$. Afterwards, we obtain a genuine, normalized density matrix by rescaling with $(\operatorname{Tr}\rho_t)^{-1}$. Therefore, we can assess the

contribution of a single trajectory $\psi_t(Z_n^*)$ to Eq. (3.25) by $\lfloor\psi_t(Z_n^*)\rfloor/N$ with

$$\lfloor\psi_t(Z_n^*)\rfloor = \sqrt{\frac{\langle\psi_t(Z_n^*),\psi_t(Z_n^*)\rangle}{\operatorname{Tr}\rho_t}}. \tag{3.26}$$

Since for the nonlinear equation the average in Eq. (3.25) is taken over normalized states $\tilde{\psi}(Z_n^*) = \psi(Z_n^*)/|\psi(Z_n^*)|$, the corresponding contribution $\lfloor\tilde{\psi}_t(Z_n^*)\rfloor/N$ is one.

Figure 3.4 shows the contribution of a few single realizations used on the left hand side of Fig. 3.3; clearly we obtain quite different results for both parameter sets. But for the weakly coupled system on the left all trajectories remain roughly in the same order of magnitude. In contrast, the contributions on the right hand side, belonging to the strongly coupled system, all vanish for large $t$, but also show pronounced peaks for a few trajectories.

We conclude, that the nonlinear hierarchy is a drastic improvement in terms of numerical efficiency for the strongly coupled system, since the additional complexity is more than compensated by the reduced sample size. Therefore, all subsequent calculations shown in this work are based on the nonlinear hierarchy unless stated otherwise.

### 3.4.2. Hierarchy Depth and Cutoff

Apart from the sample size there is an even more significant factor limiting the applicability of our hierarchical equations of motion: As seen from Fig. 3.1 the number of auxiliary states required—and with it the computational expense—grows faster then linear with the truncation depth. Before investigating the latter more thoroughly, we demonstrate the effectiveness of using an appropriate terminator instead of just truncating the hierarchy. For that matter, the Spin-Boson model is well suited since, contrary to the Dissipative two-level system presented in Sect. 2.6, it does not terminate at any finite order.

COMPLETE

# 4. Application

## 4.1. Basic Model

In the following chapter, we treat molecular aggregates with a size in the order of magnitude from a few up to a hundred molecules. Let us consider a molecule composed of electrons and point-like nuclei described quantum mechanically by canonical-conjugated pairs of operators $(p_j, q_j)$ and $(P_j, Q_j)$ respectively. The corresponding Hamiltonian is given by

$$H_{\mathrm{mol}} = T_{\mathrm{el}} + T_{\mathrm{nuc}} + U_{\mathrm{el-el}} + U_{\mathrm{nuc-nuc}} + U_{\mathrm{el-nuc}} \tag{4.1}$$

with the kinetic energies $T$ and appropriate Coulomb interactions $U$. We drop possible contributions from internal spin degrees of freedom, since they induce only negligible corrections for the systems under consideration.

The vast difference in masses of electrons and nuclei allows us to separate the dynamics of both into two individual parts using the Born-Oppenheimer approximation: As electrons move on a much faster time scale, they can respond to any changes in the nuclear arrangement almost instantaneously. This enables us to include the motion of nuclei mediated by the Coulomb potential $U_{\mathrm{el-nuc}}$ only adiabatically when calculating the electron dynamics from Eq. (4.1). Therefore, we can reorganize the summands in Eq. (4.1) more appropriately to

$$H_{\mathrm{mol}} = H_{\mathrm{el}}(\boldsymbol{Q}) + T_{\mathrm{nuc}} + U_{\mathrm{nuc-nuc}}, \tag{4.2}$$

where the notation $H_{\mathrm{el}}(\boldsymbol{Q}) = T_{\mathrm{el}} + U_{\mathrm{el-el}} + U_{\mathrm{el-nuc}}(\boldsymbol{Q})$ indicates that we regard the electronic Hamiltonian to depend only parametrically on the nuclear coordinates $\boldsymbol{Q}$. For the energy-scales under consideration, we only have to treat the valence elec-

trons explicitly; electrons on lower energy levels are included into the "environmental" nucleon-part.

The same reasoning applies to the complete Hamiltonian of the aggregate, which, besides contributions of the form (4.1) for each individual molecule, contains intermolecular interactions between electrons and nuclei in all possible combinations. Hence, it can be rephrased similarly to Eq. (4.2)

$$H_{\text{agg}} = H_{\text{el}}(\boldsymbol{Q}) + T_{\text{vib}} + U_{\text{vib−vib}}, \tag{4.3}$$

Here we use the more general notion of vibrational degrees of freedom, which not only comprises the intra- and intermolecular nuclear coordinates, but also possible environmental degrees of freedom not belonging to the aggregate. For example, the latter can be found in molecular compounds immersed in a liquid solvent.

The Born-Oppenheimer approximation allows us to analyse the electronic part separately from the vibrational part of Eq. (4.3) for a fixed set of vibrational coordinates $\boldsymbol{Q}$. Splitting up the former into contributions from each individual electron and interaction terms gives

$$H_{\text{el}} = \sum_m H_m^{(\text{el})} + \frac{1}{2} \sum_{m,n} U_{mn}^{(\text{el−el})},$$

where $H_m^{(\text{el})}$ contains the $m^{\text{th}}$ electron's kinetic energy as well as its coupling to the vibrational degrees of freedom and $U_{mn}$ is simply the Coulomb interaction between the $m^{\text{th}}$ and $n^{\text{th}}$ electron. For each given environmental configuration $\boldsymbol{Q}$, the "free" Hamiltonians $H_m^{(\text{el})}$ define adiabatic electronic eigenstates states by

$$H_m^{(\text{el})}(\boldsymbol{Q})\varphi_{ma}(q, \boldsymbol{Q}) = \epsilon_{ma}(\boldsymbol{Q})\varphi_{ma}(q, \boldsymbol{Q}).$$

Here, the index $m$ runs over all electrons under consideration and $a$ is used to label the individual states, which we assume to be ordered by the corresponding energies. Similarly to the Hartree-Fock method, we build up an expansion basis for the total electronic state by a product ansatz

$$\phi_{\boldsymbol{a}}(\boldsymbol{q}, \boldsymbol{Q}) = \prod_m \varphi_{m,a_m}(q_m, \boldsymbol{Q}), \tag{4.4}$$

which in general needs to be anti-symmetrized to fulfill the Pauli exclusion principle.

If there is at most one relevant valence electron per molecule, which is furthermore tightly bound, then the situation simplifies dramatically: In this case, the spreading of the single-electron states $|\varphi_{ma}\rangle = |m, a\rangle$ is small compared to the distance between two molecules; we can neglect the overlap $\langle m, a|n, b\rangle$ for different molecules $m \neq n$. Consequently Eq. (4.4) yields a complete basis for the electronic degrees of freedom. Expressed in this adiabatic eigen-basis the Hamiltonian (4.3) reads

$$H_{\text{el}} = \sum_{m,a} \epsilon_{m,a} |m, a\rangle\langle m, a| + \frac{1}{2} \sum_{m,n,a,b,a',b'} U_{mn}(aa', bb') |m, a; n, b\rangle\langle m, a'; n, b'|, \quad (4.5)$$

with the matrix elements of the Coulomb interaction[1]

$$U_{mn}(aa', bb') = \langle m, a; n, b|U_{mn}|m, a'; n, b'\rangle.$$

Note that all terms in Eq. (4.5) still depend on vibrational coordinates. For example the matrix elements $U_{mn}(aa'; bb')$ is influenced by the distance between the $m^{\text{th}}$ and $n^{\text{th}}$ molecule, while the electronic eigenenergies $\epsilon_{m,a}$ primarily depend on the positions of other electrons belonging to the same molecule.

In order to treat the setting described in the introduction, we do not need to consider the complete electronic Hamiltonian (4.5): If, initially, there is only a single valence electron in its lowest excited state $S_1$ above its ground state $S_0$[2] and if the various $S_0$-$S_1$-transition energies are in the same order of magnitude, then it is sufficient to take into account only the $S_0$ states $|m, 0\rangle$, as well as the first excited states $|m, 1\rangle$. Under these restrictions, the matrix elements $U_{mn}(aa', bb')$ can be classified with respect to a few physical processes such as electrostatic interactions or charge-induced transitions. The dominant contribution $U_{mn}(01; 10)$ (and its inversion $U_{mn}(10; 01)$) describes an excitation of the $n^{\text{th}}$ electron induced by a $S_1 \rightarrow S_0$ transition of the $m^{\text{th}}$ electron. In the following, we neglect all but the last classes of processes, which is frequently called Heitler-London approximation.

---

[1] This does not include the exchange interaction, since we assume vanishing mutual overlap for the electronic states.

[2] Here $S_0$ describes the lowest energy state of the valence electron with all other electrons of the molecule fixed, not to be confused with the atomic ground states.

Restricting the allowed electronic states to the two lowest energy levels has a remarkable interpretation in terms of quasi-particles: First, we define the ground state

$$|0_{\mathrm{el}}\rangle = \prod_n |n, 0\rangle \tag{4.6}$$

for the electronic system. Similarly, the product

$$|m\rangle = |m, 1\rangle \prod_{n \neq m} |n, 0\rangle \tag{4.7}$$

describes an excited electron localized in the vicinity of the $m^{\mathrm{th}}$ molecule, which we refer to as an exciton of the electronic system. By virtue of the Heitler-London approximation, our adiabatic Hamiltonian (4.5) conserves the number of excitons. Therefore, initial states $|m\rangle$ (or linear combinations thereof) remain in the one-exciton Hilbert space $\mathcal{H}^{(1)}$. The interaction matrix elements

$$V_{mn} = V_{nm} = \langle m, 0; n, 1 | U_{mn} | m, 1; n, 0 \rangle$$

allow us to express the restriction of $H_{\mathrm{el}}$ to $\mathcal{H}^{(1)}$ as

$$H_{\mathrm{el}}^{(1)}(\boldsymbol{Q}) = \sum_m \epsilon_m(\boldsymbol{Q}) |m\rangle\langle m| + \sum_{m,n} V_{mn}(\boldsymbol{Q}) |n\rangle\langle m|.$$

For the rest of this section, we assume the $V_{mn}$ to be independent of vibrational degrees of freedom; the general case is treated along the same line.

Up to this point, we have neglected the dynamical evolution of the vibrational environment, which is essential in a complete description of a molecular aggregate. Treating the environment as a bath of harmonic oscillators is sufficient for biological systems, since most proteins disintegrate at temperatures much higher than $300\,\mathrm{K}$. Therefore, thermal excitation only leads to small energy gains for each vibrational mode. Additionally, dissipation of the electronic system leads to an energy gain for the vibrational degrees of freedom. But the former is comprised only of a few valence electrons compared to the vast number of inner electrons, nucleons, etc. As energy typically spreads evenly across the environment, we can safely assume that all $Q_\lambda$ experience only a small displacement from their equilibrium positions $Q_\lambda = 0$. Thus,

the usual expansion up to second order is sufficient and yields a purely harmonic oscillator bath.

As a consequence both the site energies $\epsilon_m(\boldsymbol{Q})$ can be expanded in a Taylor series as well, neglecting all but the first non-trivial term. To alleviate notation further, we assume that each vibrational degree of freedom only couples to one specific exciton. This leads exactly to the microscopical model presented in Sect. 2.1: a bath of harmonic oscillators linearly coupled to the electronic system

$$H_{\text{agg}}^{(1)} = \sum_m \epsilon_m(0)|m\rangle\langle m| + \sum_{m,n} V_{mn}|m\rangle\langle n| + \sum_{m,\lambda} \omega_{m,\lambda} A_{m,\lambda}^\dagger A_{m,\lambda} \tag{4.8}$$
$$+ \sum_{m,\lambda} g_{m,\lambda}|m\rangle\langle m| \otimes \left( A_{m,\lambda}^\dagger + A_{m,\lambda} \right),$$

where we express the vibrational mode $\lambda$ coupling to the $m^{\text{th}}$ exciton in terms of ladder operators $A_{m,\lambda}$ and $A_{m,\lambda}^\dagger$. Throughout this chapter, we write $\epsilon_m(0) = \epsilon_m$ for the equilibrium optical transition energies. Electronic excitation are transfered from the $m^{\text{th}}$ to the $n^{\text{th}}$ molecule by virtue of the dipole-dipole interaction $V_{mn}$.

## 4.2. Transfer Dynamics

As a first exemplary application of our hierarchical equations of motion, we study energy transfer in the Fenna-Matthews-Olson (FMO) complex found in low-light adapted green sulfur bacteria. This protein complex plays a crucial role in connecting the light harvesting antenna (chlorosome) to the photosynthetic reaction center, where the absorbed solar energy is converted to a charge gradient. It is fascinating not only by virtue of its relatively small size—making it an ideal model for numerical investigation—but particularly due to the strong influence of quantum mechanical effects on the transfer, even at physiological temperature. Only lately, Engel et al. as well as Ishizaki and Fleming demonstrated that the FMO complex achieves its remarkable, almost-unit efficiency by coherent exciton motion instead of classical hopping described by Förster theory [13, 24].

The FMO protein complex is subdivided into three identical monomers, each comprising eight bacteriochlorophyll pigments (BChls). In contrast to the first seven
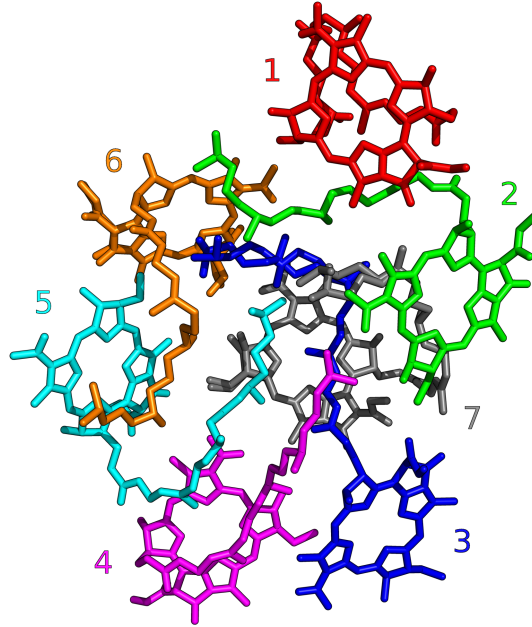
**Figure 4.1.:** Spatial structure of the simplified FMO-monomer with seven BChls []; the coloring and numbering is used throughout this section. The two main exciton-channels are $1 \rightarrow 2 \rightarrow 3$ and $6 \rightarrow 5, 7, 4 \rightarrow 3$. This figure was created using in PyMOL based on the PDB entry 3ENI [45,50].
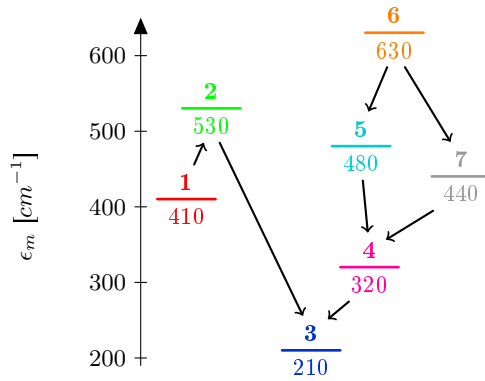


**Figure 4.2.:** Site energies of *Chlorobaculum tepidum* [1], an irrelevant global offset of $12\,000\,\mathrm{cm}^{-1}$ is subtracted. Solid black lines indicate dominant couplings leading to the two distinct transport channels.

BChls, the eighth was only discovered in recent years due to its rather weak coupling to the remaining BChls and instability during the isolation procedure in experiments [44,50]. As the main goal here is to show the applicability and reliability of our hierarchical equations of motion, we ignore BChl number eight in what follows—this simplified model has been investigated thoroughly with a vast array of methods [24,39]. For the same reason, we also restrict our attention to an individual monomer: as shown by Ritschel et al. [38], such a limitation is reasonable for the short time scales under consideration as the inter-monomeric interaction strength is rather weak.

In Fig. 4.1 we display the spatial structure and numbering of the BChls in a single monomer. The BChls 1 and 6 are situated in the vicinity of the light harvesting antenna and receive captured excitation energy, while BChl 3 acts as an energy sink to the reaction center. As both site energies $\epsilon_n$ and electronic coupling strengths $V_{mn}$ depend on the protein environment, different values for different species can be found in the literature. Here we use the data obtained from optical spectroscopy in *Chlorobaculum tepidum* [1], see Fig. 4.2 and Table B.2. Although the spectral density may be important for the details of the excitation transfer, no comprehensive information on this matter is available at present. Good agreement with experiments on *Prosthecochloris aesturaii* was achieved [36] under the semi-empirical assumption that each exciton couples to an independent environment with a Drude spectral density

$$J(\omega) = \frac{2\lambda}{\pi} \frac{\gamma\omega}{\omega^2 + \gamma^2},\tag{4.9}$$

reorganization energy $\lambda = 35\,\mathrm{cm}^{-1}$, and relaxation time $\gamma^{-1} = 50\,\mathrm{fs}$ as displayed in Fig. 4.5 A. In Sect. B.3 we calculate the corresponding bath correlation function for $T = 77\,\mathrm{K}$ and $T = 300\,\mathrm{K}$ using a Matsubara expansion. While the latter only requires a single exponential mode, we need to include a low-temperature correction mode for $T = 77\,\mathrm{K}$.

Figure 4.3 shows the results of our calculations at cryogenic temperature $T = 77\,\mathrm{K}$ using pure state hierarchy as well as the established HEOM-results of Ishizaki and Fleming [24]. Both initial excitations move remarkably fast and directed—and up to $t = 700\,\mathrm{fs}$ in a quantum-coherent, wavelike fashion—toward the energy sink at BChl 3. However, the final population of the latter is only about half as large on
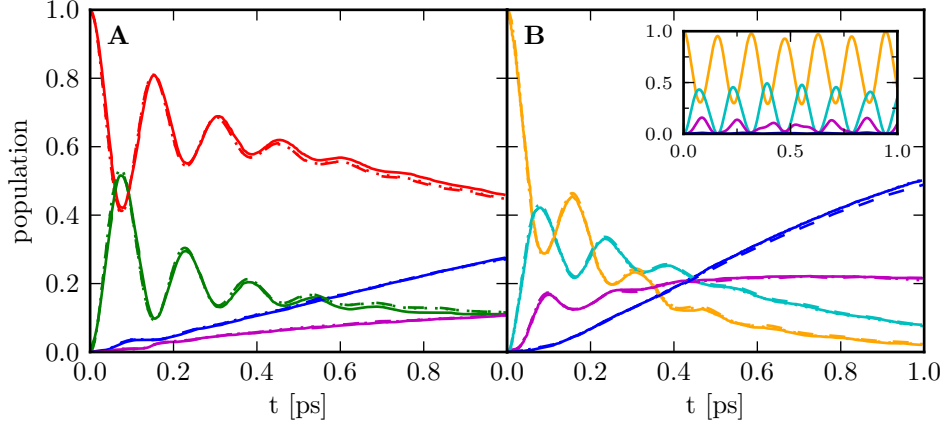
**Figure 4.3.:** Exciton transfer of the simplified FMO-monomer with seven BChls at 77 K using our stochastic hierarchical equations up to first (dotted) and second order (dashed) averaged over 10000 trajectories. For comparison, the solid line shows the results of Ishizaki and Fleming [24], which were obtained in the HEOM approach. Population for BChls 1–4 **(A)** and BChls 3–6 **(B)** with initial excitation on site 1 and 6 respectively. The inset displays a purely electronic system without coupling to the vibrational degrees of freedom. Details on parameters can be found in Sect. B.3.
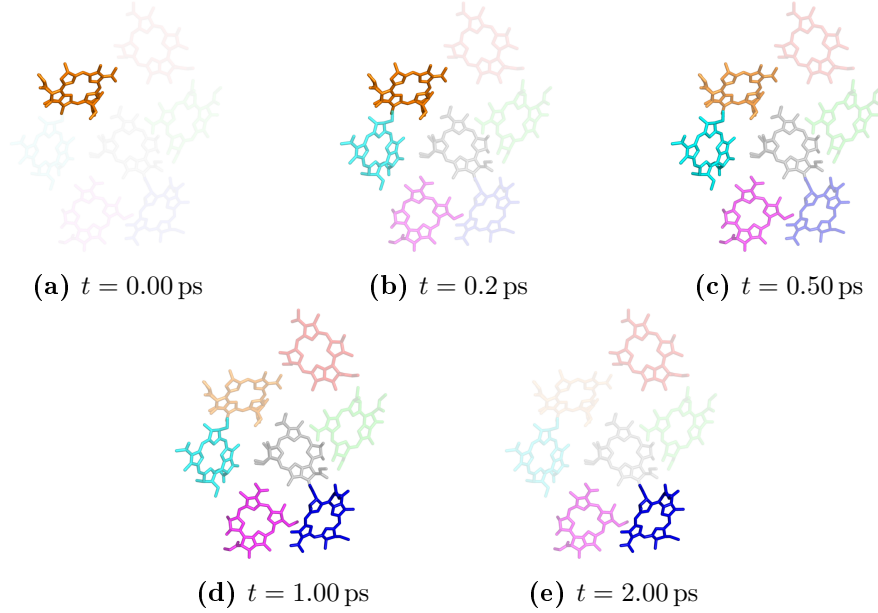


**(a)** $t = 0.00\,\text{ps}$      **(b)** $t = 0.2\,\text{ps}$      **(c)** $t = 0.50\,\text{ps}$

**(d)** $t = 1.00\,\text{ps}$      **(e)** $t = 2.00\,\text{ps}$

**Figure 4.4.:** Same as Fig. 4.3 B. The intensity of each molecule represents the population of the associated exciton state. For the sake of clarity we do not show the full molecular structure.

the left hand side due to the relatively high site energy of BChl 2. This prolongs the lifetime of an exciton-state on BChl 1 significantly, or, put differently, the electronic excitation remains on the first site for a long time. It was conjectured that this barrier is partly responsible for the high yield of the FMO-complex [24]. Indeed, the relatively small energy gap $\Delta\epsilon = 200\,\mathrm{cm}^{-1}$ between the first and third BChl is overcome quite easily by virtue of thermal excitation leading to a loss of population through this channel. The larger gap of $\Delta\epsilon = 300\,\mathrm{cm}^{-1}$ between the second and the third molecule suppresses depopulation much more efficiently. This is exactly where quantum effects influence the operation significantly: The subsidiary energetic minima at BChl 1, which would trap a classical-hopping excitation, is overcome much quicker due to quantum-mechanical delocalization.

No such initial "energy barrier" exists for the transport starting at BChl 6, therefore, the yield at BChls 3 and 4 is almost three-quarters of the total probability at $t = 1\,\mathrm{ps}$. For even longer times, all other sites show almost complete depopulation as shown in Fig. 4.4.

In the inset to Fig. 4.3 we also show the dynamics for a purely electronic system: As expected, the population-probability shows a purely oscillatory behavior with no effective excitation transport, thus emphasizing the importance of vibrational degrees of freedom in the exciton energy transfer.

Remarkably, the results of first and second order in our stochastic hierarchy are almost indistinguishable from each other and agree very well with the reference. Calculations including one more order (not shown) verify that the second order is already enough to obtain convergence in these parameter regimes. As we show in the appendix, the dominant exponential bath mode is given by[3] $g \approx (2428 - \mathrm{i}3716)\,\mathrm{cm}^{-2}$ and $\gamma \approx 106\,\mathrm{cm}^{-1}$. Therefore, the proposed truncation condition $\sqrt{g} \ll k\gamma$, which for the given parameters reads $83 \ll 106k$, might be too restricting, yet.

Nevertheless, we do not obtain complete agreement in Fig. 4.3 A for the reason discussed at the end of Sect. 3.3: As shown in the appendix, the bath correlation function of a Drude spectral density always has a discontinuous jump in its imaginary part at the origin. This manifests in the complex prefactor $g$ in our exponential mode for $t > 0$, and cannot be adjusted by the low-temperature correction term as the

---

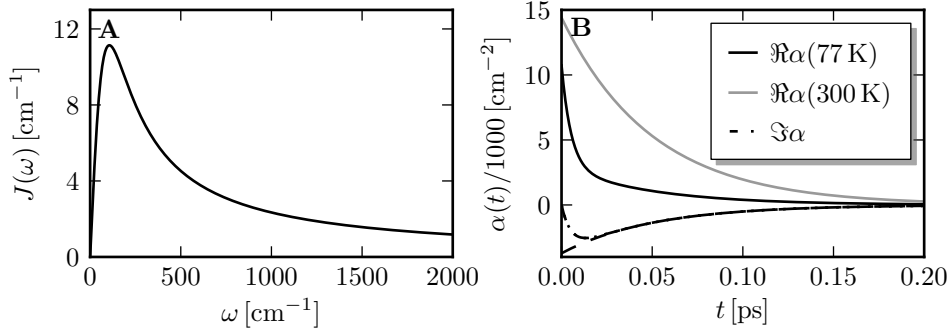[3] Recall our notation $\alpha(t) = g\mathrm{e}^{-\gamma|t|}$.

**Figure 4.5.:** Environmental parameters used for the FMO-complex. **(A)** Drude
spectral density with reorganization energy $\lambda = 35\,\text{cm}^{-1}$, and re-
laxation time $\gamma^{-1} = 50\,\text{fs}$. **(B)** Bath correlation function at $77\,\text{K}$
and $300\,\text{K}$. The imaginary part with (dotted) and without (dashed)
almost-Markovian correction is identical for both.

dashed line in Fig. 4.5 indicates. But since $\alpha$ is related to our driving processes $Z^*$
by $\alpha(t-s) = \mathbb{E}\left(Z_t Z_s^*\right)$, we cannot reproduce such a correlation function in the driving
noise. However, we approximate the discontinuous jump by including an additional,
almost-Markovian mode with purely imaginary $g$, such that $\Im\alpha(t)$ goes smoothly to
zero as $t \to 0$ while changing $\alpha$ as little as possible—the result is shown by a dotted
line in the plot. Since the low-temperature correction mode is already approximated
with an almost-Markovian mode, this does not increase the computational expense.

The exciton dynamics at physiological temperature in Fig. 4.6 shows a similar
qualitative behavior. However, the transfer is less efficient and directed, as decoher-
ence leads to a much stronger smearing of the excitation over all BChls, even the ones
not shown in this picture. For the same reason, the wave-like motion only lasts up to
$t \approx 400\,\text{fs}$. Notwithstanding, at $t = 1\,\text{ps}$ the population of the relevant, third BChl
is 0.2—still about two-thirds of the result at cryogenic temperature—and increases
further.

This time, our stochastic hierarchical equations of motion reproduce the results of
Ishizaki-Fleming almost exactly and once again, differences between first and second
order are negligible. We see in Fig. 4.5 that the imaginary part of $\alpha(0)$ is now very
small compared to its real part, therefore, the deviations it caused at $77\,\text{K}$ are not
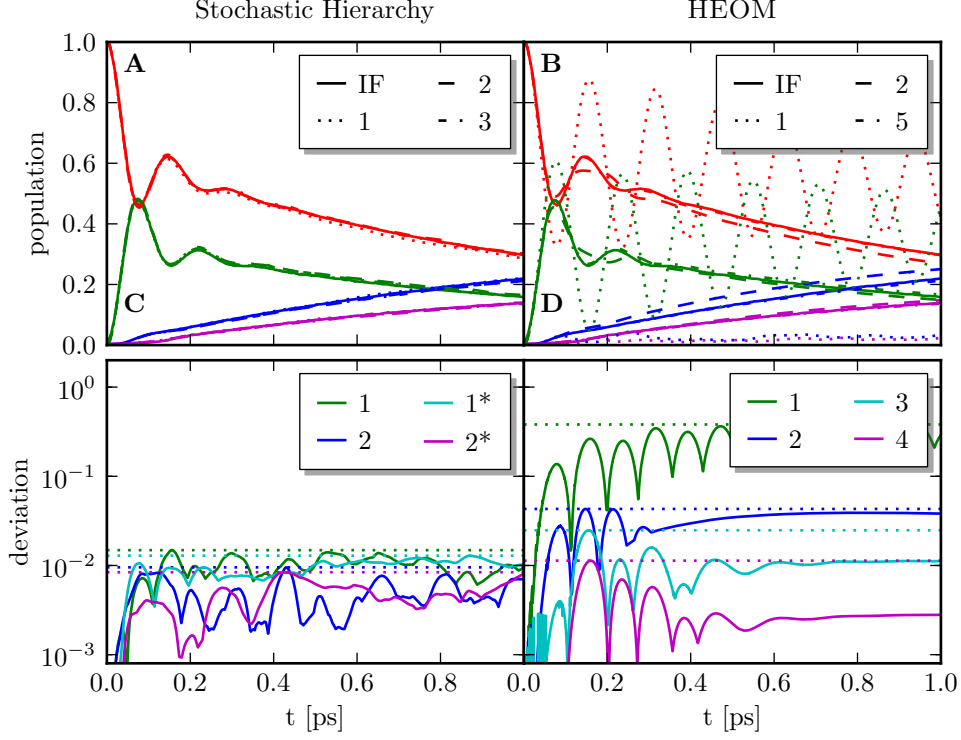
**Figure 4.6.:** Exciton transfer of the simplified FMO-monomer at 300 K and internal convergence check of the hierarchies. Solid lines are results from [24].

**(A)** Stochastic hierarchy with 10000 realizations and orders 1–3.

**(B)** Same sets of parameters, but calculated in the HEOM formalism with truncation at orders 1, 2 and 5 using PHI [49].

**(C)** The deviation of the stochastic hierarchy with respect to its third order result. Dotted lines indicate the maximum value over time. The starred curves correspond to a larger sample size of 50000 realizations.

**(D)** Same as (C), but for the HEOM calculation. Here, the reference is the fifth order result.

relevant at higher temperatures. Again, we postpone the calculations to the appendix. Nevertheless, the differences between first and second order are larger than those in the former calculation. Since the only distinction in the dominant bath mode is a larger coupling constant $g = (14279 - \mathrm{i}3716)\,\mathrm{cm}^{-1}$, this strengthens our truncation condition **??**.

On the right hand side of Fig. 4.6 B, we carry out the same calculations using the HEOM formalism [49]. Clearly, for a good approximation we need a much larger truncation order: The first order calculation displays highly undamped oscillations and the second order is necessary to get the qualitative picture right. We have found that a truncation at fifth order is necessary to correctly reproduce the coherent oscillations between $0\,\mathrm{fs}$ and $300\,\mathrm{fs}$.

To check internal convergence of each method systematically, we proceed as follows: First we define a measure for deviation of a given reduced density matrix $\rho(t) = \rho_D(t)$, obtained from a numerical calculation up to order $D$, with respect to some reference $\rho^{\mathrm{ref}}(t)$ as

$$A[\rho(t), \rho^{\mathrm{ref}}(t)] = \max_n \left| \rho_{nn}(t) - \rho_{nn}^{\mathrm{ref}}(t) \right|. \tag{4.10}$$

Since we confine our discussion to the populations of the exciton states $n$ given by $\rho_{nn}$, $A$ reflects the deviations seen in the pictures. Also, we are only interested in the convergence of a given method, therefore, the reference state $\rho^{(ref)} = \rho_D$ is calculated using the same method and selected by increasing the truncation order $D$ until $A[\rho_D(t), \rho D + 1(t)] < 10^{-2}$. This amounts to $D = 3$ for our NMSSE-hierarchy and $D = 5$ for HEOM. The accuracy of lower-order calculations with respect to the chosen reference is shown in Fig. 4.6 C and D for the stochastic and the density matrix hierarchy, respectively.

We already mentioned in the general discussion above that within the pure state hierarchy, the first order's deviation of about 2% is barely visible in Fig. 4.6 A. Although the second order approximates the result of Ishizaki-Fleming a little better, the deviation from the reference remains basically unchanged. In contrast, the same accuracy is obtained in the HEOM-formalism not until we truncate the hierarchy at third order (neglecting the stronger deviations for $t < 300\,\mathrm{fs}$), but the result converges steadily toward the reference result. Finally, the HEOM-calculations show the largest discrepancy at the initial wave-like motion and then drop off by about an order of magnitude, while the deviations of the stochastic hierarchy remain more or

less constant after $t = 0.2\,\mathrm{ps}$. All these observations combined indicate that the error of the latter is due to stochastic effects and not caused by systematic deviation. We check this statement by repeating the same calculations using a larger sample size—a star marks the corresponding results in Fig. 4.6. Clearly, they show less deviation thus confirming our assertion.

In conclusion, the discussion above shows that the hierarchical equations based on the nonlinear NMSSE provide a highly efficient method to calculate exciton energy transfer dynamics in the FMO-complex. We obtain almost perfect agreement for both, 77 K and 300 K, with the established results of Ishizaki and Fleming in first order calculations. The discrepancy of these to higher order calculations is less than a few percent, demonstrating very rapid convergence with respect to the truncation order. Of course, such an accuracy is completely unnecessary for most investigations of biological systems. The theoretical model itself is usually much less reliable due to approximations and experimental errors for the parameters involved. Also, the improved numerical efficiency, due to a reduced number of auxiliary states[4] and propagating Hilbert space vectors instead of density matrices, is more than compensated by the large sample size required. However, the stochastic hierarchies' advantages really come to fruition when dealing with more complex systems. For example, data from fluorescence line-narrowing measurements on *Prosthecochloris aesturaii* indicate that realistic spectral densities are far more structured, requiring as much as 25 exponential modes This amounts to 176 auxiliary states for $D = 1$ compared to a tremendous number of 41 million states required by a fourth-order calculation.

## 4.3. Absorption Spectra

The second exemplary application of our pure-state hierarchy is the calculation of absorption spectra in molecular aggregates. In general, the NMSSE provides a highly efficient framework to attack this problem, since all the relevant information is encoded in a single realization $\psi_t(Z^* = 0)$ and no stochastic average is necessary. In previous work based on the convolutionless formulation (2.16) in ZOFE approximation, good agreement with the exact pseudo-mode approach was achieved in large

---

[4]In the case of a single bath mode, we have eight auxiliary states for $D = 1$ compared to 330 for $D = 4$.

parts of the parameter space [42]. However, for intermediate values of the electronic coupling $V_{mn}$ noticeable deviations occurred. Here, we show that the linear hierarchy (3.7) provides an efficient tool to calculate spectra even for large systems with a highly-structured spectral density.

### 4.3.1. NMSSE for Spectra

In this section, we demonstrate the simple connection between solutions of the linear NMSSE with $Z_t^* = 0$ and absorption spectra of molecular aggregate at zero temperature [41, 42]. Using the thermo-field construction from Sect. 2.5, we can treat an arbitrary thermal environment along the same lines [].

Clearly, for $T = 0\,\mathrm{K}$ the initial state of the aggregate is given by $|0_{\mathrm{el}}\rangle \otimes |0\rangle$ with the electronic ground state $|0_{\mathrm{el}}\rangle$ defined in Eq. (4.6) and the vibrational ground state $|0\rangle$. In dipole-approximation the absorption coefficient of light with frequency $\nu$ and polarization $\vec{E}$ is given by [30]

$$A(\nu) = \Re \left( \int_0^\infty \mathrm{e}^{\mathrm{i}\nu t} M(t)\, \mathrm{d}t \right), \tag{4.11}$$

where the dipole-correlation function reads

$$M(t) = \langle 0_{\mathrm{el}}|\langle 0|\vec{\mu} \cdot \vec{E}\, \mathrm{e}^{-\mathrm{i}H_{\mathrm{agg}}t}\, \vec{\mu} \cdot \vec{E}^*|0_{\mathrm{el}}\rangle|0\rangle \tag{4.12}$$

Here, $\vec{\mu} = \sum_m \vec{\mu}_m$ denotes the total dipole operator of the aggregate and $H_{\mathrm{agg}} = H_{\mathrm{agg}}^{(0)} + H_{\mathrm{agg}}^{(1)}$ is the total aggregate Hamiltonian restricted to the electronic subspace with at most one exciton. Its single-exciton contribution is given by Eq. (4.8). Provided the dipole-operators are independent of the vibrational degrees of freedom, inserting complete sets of electronic basis vectors $\sum_m |m\rangle\langle m|$ in Eq. (4.12) yields

$$M(t) = \sum_{m,n} d_m^* d_n\, \langle m|\langle 0|\mathrm{e}^{-\mathrm{i}H_{\mathrm{agg}}t}|n\rangle|0\rangle \tag{4.13}$$

with the transition dipole-elements projected in the direction of polarization

$$d_m = \langle m|\vec{\mu} \cdot \vec{E}^*|0_{\mathrm{el}}\rangle.$$

Since the expectation-value of the time-evolution operator in Eq. (4.13) includes only

contributions from the one-exciton subspace, it is equivalent to

$$M(t) = \left( \sum_m d_m^* \langle m| \langle 0| \right) e^{-iH_{\mathrm{agg}}^{(1)}t} \left( \sum_n d_n |n\rangle |0\rangle \right) = |\boldsymbol{d}|^2 \langle \Psi_0 | \Psi_t \rangle.$$

Here, $|\Psi_t\rangle$ denotes the solution to

$$\partial_t |\Psi_t\rangle = -iH_{\mathrm{agg}}^{(1)} |\Psi_t\rangle, \qquad |\Psi_0\rangle = |\psi_0\rangle \otimes |0\rangle \tag{4.14}$$

with the initial electronic state $|\psi_0\rangle = |\boldsymbol{d}|^{-1} \sum_m d_m |m\rangle$. The sum of the dipole-elements $|\boldsymbol{d}|^2 = \sum_n |d_n|^2$ is introduced to ensure normalization of $|\psi_0\rangle$.

Equation (4.14) is already very close to the microscopical version of our NMSSE. The only difference to Eq. (2.11) is that the latter is formulated in the interaction picture. However, $\langle \Psi_0 | \Psi_t \rangle$ does not change under the transformation to the interaction picture, since the environmental vacuum is an eigenstate of $H_{\mathrm{env}}$ with eigenvalue 0. Therefore, we can insert the resolution of unity for coherent states (2.9) and obtain

$$M(t) = |\boldsymbol{d}|^2 \int \frac{\mathrm{d}^{2N}z}{\pi^N} \langle \psi_0 | \psi_t(\boldsymbol{z}^*) \rangle \langle 0 | \boldsymbol{z} \rangle,$$

where $\psi_t(\boldsymbol{z}^*)$ is the solution to Eq. (2.11). As $\langle 0 | \boldsymbol{z} \rangle = 1$ and $\langle \psi_0 | \psi_t(\boldsymbol{z}^*) \rangle$ is analytical in $\boldsymbol{z}^*$, the only term of the corresponding Taylor series that is not canceled by the integral is independent of $\boldsymbol{z}^*$. In other words, the dipole correlation function expressed in terms of solutions $\psi_t(Z^*)$ of the linear NMSSE reads

$$M(t) = |\boldsymbol{d}|^2 \langle \psi_0 | \psi_t(\boldsymbol{z}^* = 0) \rangle = |\boldsymbol{d}|^2 \langle \psi_0 | \psi_t(Z^* = 0) \rangle \tag{4.15}$$

Of course, this does not imply that we can simply drop the functional derivative from the NMSSE. Nevertheless, the corresponding hierarchy (3.7) is completely local in $Z_t^*$, so we can set $Z_t^* = 0$ in each order. In conclusion, assuming a single exponential bath mode $\alpha(t) = g\, e^{-(\gamma + i\Omega)t}$ $(t > 0)$, the relevant trajectory $\psi_t(Z^* = 0) =: \psi_t^{(0)}$ satisfies the following set of equations

$$\partial_t \psi_t^{(k)} = (-iH - (\gamma + i\Omega)\psi_t^{(k)} + k\alpha(0)\psi_t^{(k-1)} - L^\dagger \psi_t^{(k+1)}. \tag{4.16}$$

59

with initial conditions $\psi_0^{(0)} = \psi_0$ and $\psi_0^{(k)} = 0$ $(k \geq 1)$.

### 4.3.2. Results

As a first test, we investigate absorption spectra of linear aggregates with identical monomers and parallel dipole-moments. For the electronic interaction, we assume nearest-neighbor coupling $V_{mn} = V\delta_{m,n+1} + V\delta{m,n-1}$ with equal strength. The vibrational degrees of freedom are described by a single exponential mode $\alpha(t) = \mathrm{e}^{-\gamma|t| - \mathrm{i}\Omega t}$. We use the results of Roden, Strunz and Eisfeld [42] obtained in the exact pseuo-mode approach as a reference, but also compare a few aspects to the ZOFE-results from the same work.

Figure 4.7 displays the spectra of a dimer for two widths of the spectral density, namely $\gamma = 0.25\,\Omega$ and $\gamma = 0.1\,\Omega$, and different values for the coupling strength $V$. With truncation order $D = 5$ (dashed line), we obtain perfect agreement with the reference for all values of $V$. To investigate the behavior for smaller truncation orders, we also show the results for $D = 1$ (solid) and $D = 3$ (dotted). Not surprising, these approximate the exact result better for the larger $\gamma = 0.25$ compared to $\gamma = 0.1$. Similar to the ZOFE-approach, the best agreement with any truncation order is achieved for large values of $|V|$, because the impact of the environment is reduced by a strong electronic Hamiltonian. For smaller $|V|$, the influence of the environment grows and more orders are needed in order to reproduce the reference's results. However, there is an important difference to the behavior of the ZOFE-calculations: While the latter is exact for $V = 0$ [42], the deviation of the first order NMSSE-hierarchy is even more pronounced compared to $V = -0.41$.

We now discuss a major advantage of the NMSSE-hierarchy over the pseudo-mode approach. Already Fig. 4.7 shows that the first order calculations are always sufficient to reproduce the position of lowest energy peak up to very high precision. Even the shape and magnitude of the latter fit well to the exact result in most cases. This behavior continues for the next peaks, too, as the pictures corresponding to $V = 0.44$ show: Although the higher-frequency spectrum $\nu > 0$ is obtained only with the maximum value $k = 5$ for the truncation order, the position of the second peak is well-approximated at the intermediate value $D = 3$.

To strengthen this statement, we study a more complex system, namely a PTCDA
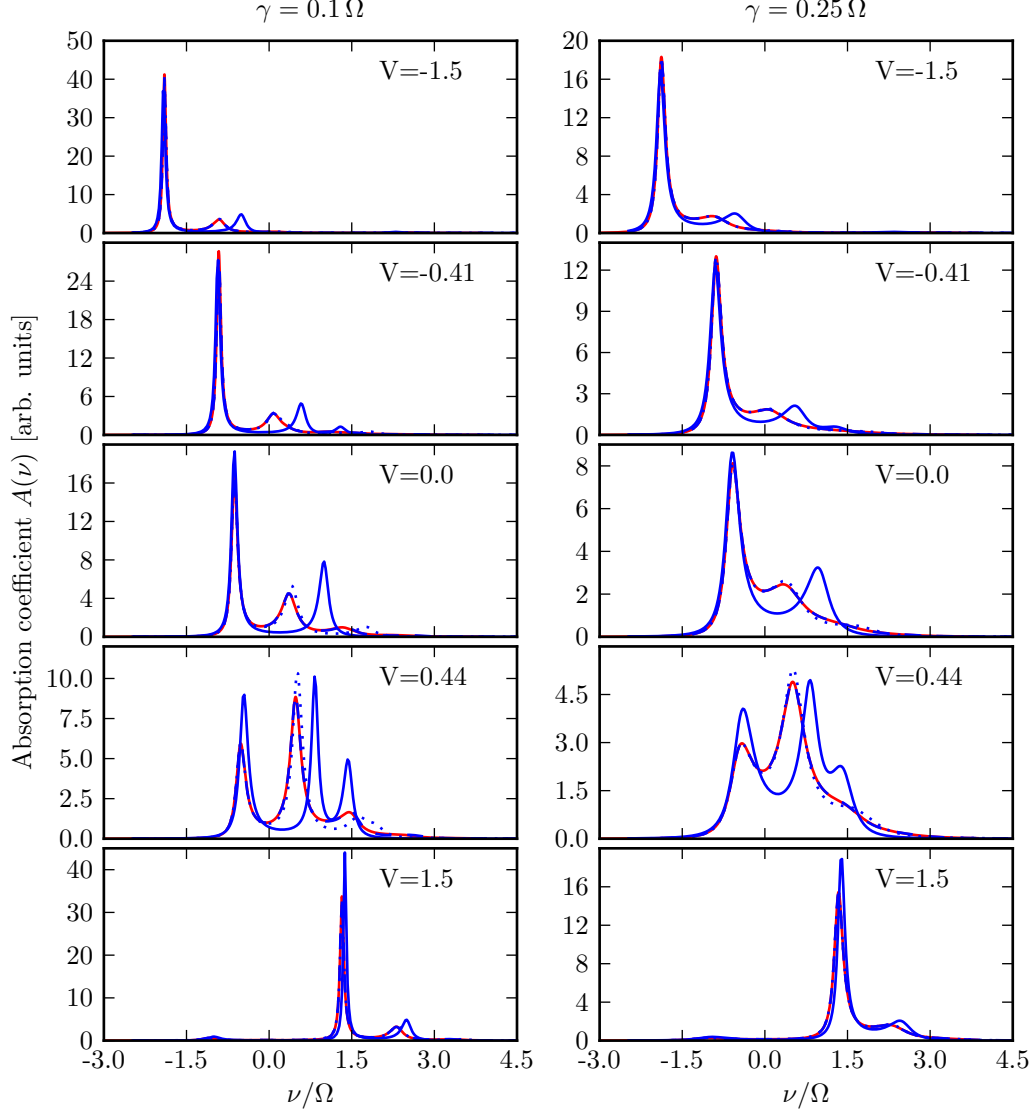
**Figure 4.7.:** *Left column*: Absorption spectra for a Dimer and a single exponential bath mode with $g = 0.64\Omega^2$ and $\gamma = 0.1\Omega$.
*Right column*: Same, but with $\gamma = 0.25\Omega$.
We compare the NMSSE-hierarchy (blue) truncated at first (solid), third (dotted) and fifth (dashed) order to the pseudo-mode results (red).
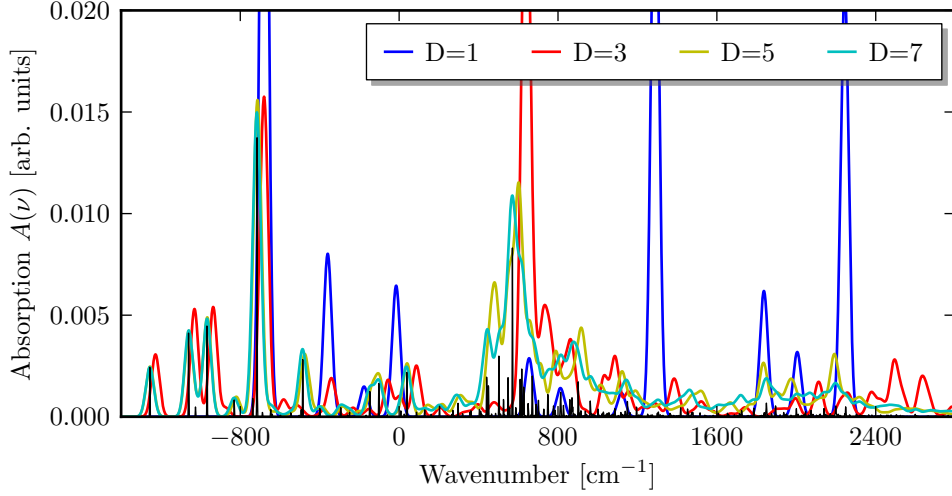
**Figure 4.8.:** Absorption spectrum for the PTCDA-dimer convoluted with a Gaussian of width $\sigma = 20\,\mathrm{cm}^{-1}$ with electronic coupling $V = 600\,\mathrm{cm}^{-1}$ and different truncation orders $D$ of the hierarchy. The black lines display the sharp peaks of spectrum for $D = 7$ with a much narrower enveloping Gaussian ($\sigma = 1\,\mathrm{cm}^{-1}$). We use a bath correlation function with six purely-oscillatory exponentials, see **??** for the parameters [40, Tab. 1 D].

dimer with a bath correlation function consisting of six exponential modes. The latter was already used as an approximation to a realistic environment in pseudo-mode calculations [40]. In contrast to the rest of this work, all modes under consideration are purely oscillatory, that is $\gamma = 0$. Nevertheless, Fig. 4.8 clearly shows a behavior similar to the previous spectra 4.7 with increasing truncation order $D$: Even the first order $D = 1$ yields the correct position of the lowest major peak at wavenumber $k \approx -800\,\mathrm{cm}^{-1}$ with good precision, but fails at higher energies. The next higher order shown $(D = 3)$ roughly reproduces the correct magnitude and position for the three characteristic peaks on the left and approximately indicates the smaller structure between the two major peaks at $k \approx -800\,\mathrm{cm}^{-1}$ and $k \approx 700\,\mathrm{cm}^{-1}$. The latter marks the upper boundary for the region where the two highest order calculations $D = 5$ and $D = 7$ practically coincide. For even higher wavenumber, deviations are pronouncedly visible but not random. Roughly, the highest order calculation only improves the position and magnitude of the peaks that are already present for $D = 5$.

Summarizing the above, we have demonstrated that the hierarchy of pure states provides an efficient tool to study absorption spectra of quantum aggregates. In contrast to the study of transfer and dynamics, the calculation of spectra in the NMSSE requires no Monte-Carlo average over several realizations. Therefore, one major advantage of the NMSSE compared to density-matrix formalisms, namely the propagation of state vectors, really comes into its one. This combined with the very predictable behavior for a growing number of hierarchy orders allows studying large-dimensional systems coupled to a highly structured environment, especially in the small-wavenumber regime. Besides, we have also demonstrated that truncation of the NMSSE-hierarchy is possible for $\gamma \to 0$, exemplifying applicability of this approach even the highly non-Markovian limit.

# 5. Conclusions

<span style="color:red">CONCLUSION</span>

# A. Analytic Solution of the Jaynes-Cummings Model

## A.1. General Approach

Here we present in full detail the analytic solution of the Jaynes-Cummings model introduced in Sect. 2.6. For zero-temperature the relevant NMSSE can always be expressed in terms of a single process

$$\partial_t \psi_t = -\mathrm{i}\frac{\omega}{2}\sigma_z \psi_t + g\sigma_- Z_t^* \psi_t - g\sigma_+ \int \alpha(t-s)\frac{\delta\psi_t}{\delta Z_s^*}\,\mathrm{d}s. \tag{A.1}$$

We make an ansatz for the quantum trajectory at most linear in $Z_s^*$

$$\psi_t(Z^*) = \psi(t) + \int_0^t \psi_s(t) Z_s^*\,\mathrm{d}s. \tag{A.2}$$

Here we already incorporate the $Z_s^*$-independence of $\psi_t(Z^*)$ for $s < 0$ and $s > t$ using a bounded integral domain.[1] The "+"-component of our NMSSE with the ansatz (A.2) reads

$$\dot{\psi}^+(t) + \psi_t^+(t) Z_t^* + \int_0^t \dot{\psi}_s^+ Z_s^*\,\mathrm{d}s$$
$$= -\mathrm{i}\frac{\omega}{2}\left(\psi^+(t) + \int_0^t \psi_s^+(t) Z_s^*\,\mathrm{d}s\right) - g\int_0^t \alpha(t-s)\psi_s^-(t)\,\mathrm{d}s. \tag{A.3}$$

---

[1] A consistent treatment of these independence-conditions is more tricky than it seems at first glance, since we are mixing a distributional object $Z_s^*$ with a discontinuous function $s \mapsto \psi_s(t)$. As $\delta\psi_t(Z^*)/\delta Z_s^* = 0$ translates to $\psi_s(t) = 0$, the correct integral boundary reads $\int_{0-\varepsilon}^{t+\varepsilon}$ with $\varepsilon > 0$ but arbitrary otherwise.

In order to separate contributions of different order in $Z_s^*$, we apply the functional derivative $\delta/\delta Z_s^*$ to the last equation

$$\psi_t^+(t)\delta(t-s) + \int_0^t \dot{\psi}_{s'}^+(t)\delta(s-s')\,\mathrm{d}s' = -\mathrm{i}\frac{\omega}{2}\int_0^t \psi_{s'}^+(t)\delta(s-s')\,\mathrm{d}s'. \qquad (A.4)$$

Choosing $s \in (0,t)$ leaves us with a simple ordinary differential equation with solution $\psi_s^+(t) = C_s\exp(-\mathrm{i}\omega t/2)$. Since there is only one singular term in Eq. (A.4), $\psi_s^+(s)$ and thus the constant $C_s$ must vanish. This amounts formally to integrating (A.4) over a small interval $(t-\varepsilon, t+\varepsilon)$ with respect to $s$. In the limit $\varepsilon \to 0$ all terms except the first go to zero.

On the other hand we can isolate all terms independent of $Z_s^*$ in Eq. (A.3) simply by taking the expectation value, yielding

$$\dot{\psi}^+(t) = -\mathrm{i}\frac{\omega}{2}\psi^+(t) - g\int_0^t \alpha(t-s)\psi_s^-(t)\,\mathrm{d}s. \qquad (A.5)$$

We postpone its solution to the end of this section.

The "-" component of Eq. (A.1) is quite similar to (A.3):

$$\dot{\psi}^-(t) + \psi_t^-(t)Z_t^* + \int_0^t \dot{\psi}_s^-(t)Z_s^*\,\mathrm{d}s$$
$$= \mathrm{i}\frac{\omega}{2}\left(\psi^-(t) + \int_0^t \psi_s^-(t)Z_s^*\right) + g\psi^+(t)Z_t^*, \qquad (A.6)$$

where we already used that $\psi_s^+(t) = 0$. All terms independent of $Z^*$ require

$$\psi^-(t) = \psi^-(0)\,\mathrm{e}^{\mathrm{i}\frac{\omega}{2}t}. \qquad (A.7)$$

In the same manner as we derived Eq. (A.4), we can treat all terms proportional to $Z_t^*$; again we find a solution of the form $\psi_s^-(t) = C_s\exp(\mathrm{i}\omega t/2)$; the only difference is an additional singular term due to the driving process in Eq. (A.1). It gives rise to the boundary condition $\psi_t^-(t) = g\psi^+(t)$; therefore Together with **??** we obtain a closed equation for $\psi^+(t)$

$$\dot{\psi}^+(t) = -\mathrm{i}\frac{\omega}{2}\psi^+(t) - c^2\int_0^t \alpha(t-s)\mathrm{e}^{\mathrm{i}\frac{\omega}{2}(t-s)}\psi^+(s)\,\mathrm{d}s. \qquad (A.8)$$

Hence we may replace the original NMSSE (A.1) by a $\mathbb{C}$-valued integro-differential equation. The full solution to Eq. (A.1) in terms of $\psi^+(t)$ is written out in Eq. (2.52).

## A.2. Exponential Correlation Function

Equation (A.8) still contains a memory integral, which appears to be impossible to solve analytically for an arbitrary bath correlation function. The situation is noticeably simpler for

$$\alpha(t-s) = \sum_{j=1}^{N} g_j \, \mathrm{e}^{-\gamma_j|t-s|-\mathrm{i}\Omega_j(t-s)}. \tag{A.9}$$

Since $\psi^+$ only depends on values of $\alpha(t)$ for $t \geq 0$ we can assume $\gamma = 0$ without loss of generality. Similar to our hierarchical equations of motion we absorb the problematic terms into auxiliary functions

$$\phi_j(t) := \int_0^t \alpha_j(t-s)\mathrm{e}^{\mathrm{i}\frac{\omega}{2}(t-s)}\psi^+(s) \, \mathrm{d}s, \tag{A.10}$$

this allows us to rewrite Eq. (A.8) as a system of $(N+1)$ ordinary differential equations

$$\dot{\psi}^+(t) = -\mathrm{i}\frac{\omega}{2}\psi^+(t) - g^2 \sum_{j=1}^{N} \phi_j(t)$$

$$\dot{\phi}_j(t) = g_j\psi^+(t) + \mathrm{i}\left(\frac{\omega}{2} - \Omega\right)\phi_j(t).$$

with constant coefficients and initial conditions $\psi^+(0)$ as well as $\phi_j(0) = 0$. In the special case $N = 1$ the diagonalization of the coefficient matrix can be carried out analytically; for $N = 2$ it is—at least in principle—possible, too. With the shorthand notation $\tilde{\Omega} = \sqrt{(\omega-\Omega)^2 + 4g^2}$ and $g_1$ absorbed into the coupling strength $g$, the solution to Eq. (A.8) reads

$$\psi^+(t) = \frac{\psi^+(0)}{2\tilde{\Omega}}\left((\omega-\Omega+\tilde{\Omega})\,\mathrm{e}^{-\mathrm{i}\frac{\Omega+\tilde{\Omega}}{2}t} - (\omega-\Omega-\tilde{\Omega})\,\mathrm{e}^{-\mathrm{i}\frac{\Omega-\tilde{\Omega}}{2}t}\right). \tag{A.11}$$

# B. Some Remarks concerning the Hierachy

## B.1. The Memory-Integral Term

In this section we discuss the crucial simplification, how an exponential bath correlation function $\alpha(t) = g\,\mathrm{e}^{-\gamma|t|-\mathrm{i}\Omega t}$ leads to

$$\dot{\mathcal{D}}_t \psi_t(Z^*) = (-\gamma + \mathrm{i}\Omega)\mathcal{D}_t \psi_t(Z^*) \tag{B.1}$$

for the noise-derivation operator $\mathcal{D}_t = \int \alpha(t-s)\delta/\delta Z_s^*$ applied to a solution of the NMSSE with vacuum initial conditions, that is $\frac{\delta\psi_0}{\delta Z_s^*} = 0$.

For the above $\dot{\mathcal{D}}_t = \int \dot\alpha(t-s)\delta/\delta Z_s^*$, we need to calculate

$$\dot\alpha(t) = g\mathrm{e}^{-\mathrm{i}\Omega t}\left((-\gamma - \mathrm{i}\Omega)\Theta(t)\mathrm{e}^{-\gamma t} + (\gamma - \mathrm{i}\Omega)\Theta(-t)\mathrm{e}^{\gamma t}\right). \tag{B.2}$$

Notice that the singular time-derivatives $\dot\Theta = \delta$ cancel. This show clearly, that $\dot{\mathcal{D}}_t \sim \mathcal{D}_t$ does not hold on the level of operators. Even the vanishing of the functional derivative $\delta\phi_t(Z^*)/\delta Z_s^*$ for $s > t$ with some arbitrary stochastic state $\phi_t(Z^*)$ does not imply $\dot{\mathcal{D}}_t\phi_t(Z^*) \sim \mathcal{D}_t\phi_t(Z^*)$ as the following example shows: Take a noise expansion of the form $\phi_t(Z^*) = \varphi \cdot (Z_t^* + Z_{t'}^*)$, where $\varphi$ is some $Z_t^*$ independent system state and $0 < t' < t$. It clearly satisfies the required boundary conditions, but

$$\dot{\mathcal{D}}_t\phi_t(Z^*) = (\dot\alpha(0) + \dot\alpha(t-t'))\varphi = \left(-2\mathrm{i}\Omega - (\gamma + \mathrm{i}\Omega)\mathrm{e}^{-(\gamma+\mathrm{i}\Omega)(t-t')}\right)\varphi$$

which is not proportional to

$$\mathcal{D}_t\phi_t(Z^*) = (\alpha(0) + \alpha(t-t'))\varphi = g(1 + \exp(-\gamma + \mathrm{i}\Omega)(t-t'))\varphi.$$

The problematic first summand arises due to singular behavior of $\delta\phi_t(Z^*)/\delta Z_s^*$ at the

upper integral bound $s = t$.

However, such problems do not occur once we restrict $\dot{\mathcal{D}}_t$ to solutions of our NMSSE (3.1) with vacuum initial conditions. Indeed, since $\delta\psi_t/\delta Z_t^* \sim L\psi_t$, the functional derivative of $\psi_t(Z^*)$ at the upper bound is regular and therefore has vanishing weight under the integral. This is how we obtain Eq. (B.1).

## B.2. Terminating the Hierarchy

$$\psi_t^{(k)} = \int_0^t e^{-kw(t-s)} \, T_+ \, e^{\int_s^t -iH + LZ_u^* \, \mathrm{d}u} \left( k\alpha(0) L\psi_s^{(k-1)} - L^\dagger \psi_s^{(k+1)} \right) \mathrm{d}s, \qquad \text{(B.3)}$$

## B.3. Application to FMO

In this section we present the details for the FMO-transfer in Sect. 4.2. We start by calculating the exponential expansion

$$\alpha(t) = \sum_{n=0}^{\infty} g_n \, e^{-\gamma_n t} \qquad \text{(B.4)}$$

of the bath correlation function for a Drude spectral density

$$J(\omega) = \frac{2\lambda}{\pi} \frac{\gamma\omega}{\omega^2 + \gamma^2}$$

with poles $\omega = \pm i\gamma$ and residues $\text{Res}_{\pm i\gamma}(J) = \frac{\gamma\lambda}{\pi}$. Let us write $\alpha(t) = a(t) + ib(t)$ with the corresponding integrals

$$a(t) = \frac{1}{2} \int J(\omega) \coth\left(\frac{\beta\omega}{2}\right) e^{i\omega t} \, \mathrm{d}\omega \qquad \text{and} \qquad b(t) = \frac{1}{2i} \int J(\omega) \, e^{i\omega t} \, \mathrm{d}\omega.$$

As already mentioned in Sect. 3.3, these integrals are solved using the residue theorem: For $t > 0$ we have to include only poles with positive imaginary part, so

Eq. (3.23) gives

$$a(t) = \mathrm{i}\gamma\lambda \coth\left(\frac{\mathrm{i}\beta\gamma}{2}\right) \mathrm{e}^{-\gamma t} + \frac{2\pi\mathrm{i}}{\beta} \sum_{\gamma_n} \frac{2\lambda}{\pi} \frac{\mathrm{i}\gamma\gamma_n}{-\gamma_n^2 + \gamma^2} \mathrm{e}^{-\gamma_n t}$$
$$= \gamma\lambda \cot\left(\frac{\beta\gamma}{2}\right) \mathrm{e}^{-\gamma t} + \frac{4\lambda\gamma}{\beta} \sum_{\gamma_n} \frac{\gamma_n}{\gamma_n^2 - \gamma^2} \mathrm{e}^{-\gamma_n t},$$

where the last sum is taken over Matsubara frequencies $\gamma_n = 2\pi n/\beta$, $n \geq 1$. For convenience we also set $\gamma_0 = \gamma$.

Similarly, we have for the imaginary part

$$b(t) = \gamma\lambda\, \mathrm{e}^{-\gamma t}.$$

In conclusion, we obtain for the parameters in the expansion (B.4)

$$g_0 = \gamma\lambda\left(\cot\left(\frac{\beta\gamma}{2}\right) - \mathrm{i}\right) \qquad \text{and} \qquad g_{n\geq 1} = \frac{4\lambda\gamma}{\beta} \frac{\gamma_n}{\gamma_n^2 - \gamma^2}.$$

We now turn to the concrete values used in Sect. 4.2 and the calculations of Ishizaki-Fleming [24]; for the results see Table B.1.

Compared to the inverse relaxation time $\gamma_0 = 106\,\mathrm{cm}^{-1}$, the first Matsubara frequency $\gamma_1 = 1310\,\mathrm{cm}^{-1}$ at $T = 300\,\mathrm{K}$ is already quite large. The opposite holds for the corresponding coupling strengths $g_0 = (14279 - 3716\mathrm{i})\,\mathrm{cm}^{-2}$ and $g_1 = 2381\,\mathrm{cm}^{-2}$, respectively. Hence, we follow the reference and drop all low-temperature correction terms with $n \geq 1$ in Eq. (B.4).

For cryogenic temperature $T = 77\,\mathrm{K}$, a single mode with $g_0 = (2916 - 3716\mathrm{i})\,\mathrm{cm}^{-2}$ is not sufficient, since the first low-temperature correction term is given by $\gamma_1 = 336\,\mathrm{cm}^{-2}$ and $g_1 = 2628\,\mathrm{cm}^{-2}$. However, the latter was approximated by a purely Markovian mode $\gamma_1\, \mathrm{e}^{-\gamma_1 t} \approx \delta(t)$ by Ishizaki-Fleming in order to keep the number of modes as small as possible for the HEOM-approach. The implementation of the pure-state hierarchies could not handle a true Markovian mode, so we resort to an exponential mode with $\tilde{\gamma}_1 > 1000\,\mathrm{cm}^{-1}$ in order to obtain good agreement. To check whether such an approximation has a large impact on the results, we also check the true values in ??

73

| | Fig. 4.3 | Fig. 4.6 | ?? |
|---|---|---|---|
| $g_0$ [cm$^{-2}$] | $2916 - 3716i$ | $14279 - 3716i$ | $2916 - 3716i$ |
| $\gamma_0$ [cm$^{-1}$] | 106 | 106 | 106 |
| $g_1$ [cm$^{-2}$] | 7814* | – | 2628 |
| $\gamma_1$ [cm$^{-1}$] | 1000* | – | 336 |
| $g_2$ [cm$^{-2}$] | 3716i | 3716i | 3716i |
| $\gamma_2$ [cm$^{-1}$] | 1000 | 1000 | 1000 |

**Table B.1.:** Parameters for the bath correlation function $\alpha(t) = \sum_n g_n \, \mathrm{e}^{-\gamma_n t}$ used in Sect. 4.2. Values marked with a star are approximated Markov-modes from the reference. The third mode is merely used to remove the imaginary part of $\alpha(0)$.

| $H_{mn}$ [cm$^{-1}$] | 1 | 2 | 3 | 4 | 5 | 6 | 7 |
|---|---|---|---|---|---|---|---|
| 1 | **410** | -87.7 | 5.5 | -5.9 | 6.7 | -13.7 | -9.9 |
| 2 | | **530** | 30.8 | 8.2 | 0.7 | 11.8 | 4.3 |
| 3 | | | **210** | -53.5 | -2.2 | -9.6 | 6.0 |
| 4 | | | | **320** | -70.7 | -17.0 | -63.3 |
| 5 | | | | | **480** | 81.1 | -1.3 |
| 6 | | | | | | **630** | 39.7 |
| 7 | | | | | | | **440** |

**Table B.2.:** Matrix elements of the purely electronic Hamiltonian used in Sect. 4.2. Consists of site energies (bold) and electronic coupling elements for *Chlorobaculum tepidum* [1]. An irrelevant global offset of $12\,000\,\mathrm{cm}^{-1}$ has been subtracted from the site energies.

# Bibliography

[1] Julia Adolphs and Thomas Renger. How proteins trigger excitation energy transfer in the fmo complex of green sulfur bacteria. *Biophysical journal*, 91(8):2778–2797, 2006.

[2] R Alicki and K Lendi. Quantum dynamical semigroups and applicationsspringer. *Berlin, Heidelberg*, 1987.

[3] Alberto Barchielli and Matteo Gregoratti. *Quantum trajectories and measurements in continuous time: the diffusive case*, volume 782. Springer, 2009.

[4] V. Bargmann. On a hilbert space of analytic functions and an associated integral transform part i. *Communications on Pure and Applied Mathematics*, 14(3):187–214, 1961.

[5] Ola Bratteli and Derek W Robinson. *Operator algebras and quantum statistical mechanics 1: C\*-and W\*-algebras. Symmetry groups. Decomposition of states*, volume 1. Springer, 2003.

[6] H.P. Breuer and F. Petruccione. *The Theory of Open Quantum Systems*. Oxford University Press on Demand, 2002.

[7] A.O Caldeira and A.J Leggett. Quantum tunnelling in a dissipative system. *Annals of Physics*, 149(2):374 – 456, 1983.

[8] H. Carmichael. *An Open Systems Approach to Quantum Optics: Lectures Presented at the Université Libre de Bruxelles, October 28 to November 4, 1991*. Lecture Notes in Computer Science. Springer Berlin Heidelberg, 1993.

[9] Lajos Diósi. Exact semiclassical wave equation for stochastic quantum optics. *Quantum and Semiclassical Optics: Journal of the European Optical Society Part B*, 8(1):309, 1996.

[10] Lajos Diósi, Nicolas Gisin, and Walter T. Strunz. Non-markovian quantum state diffusion. *Phys. Rev. A*, 58:1699–1712, Sep 1998.

[11] Lajos Diósi and Walter T. Strunz. The non-markovian stochastic schrödinger equation for open systems. *Physics Letters A*, 235(6):569 – 573, 1997.

[12] William L Dunn and J Kenneth Shultis. *Exploring Monte Carlo Methods.* Access Online via Elsevier, 2011.

[13] Gregory S Engel, Tessa R Calhoun, Elizabeth L Read, Tae-Kyu Ahn, Tomáš Mančal, Yuan-Chung Cheng, Robert E Blankenship, and Graham R Fleming. Evidence for wavelike energy transfer through quantum coherence in photosynthetic systems. *Nature*, 446(7137):782–786, 2007.

[14] Richard Phillips Feynman and Frank Lee Vernon. The theory of a general quantum system interacting with a linear dissipative system. *Annals of physics*, 24:118–173, 1963.

[15] R.P. Feynman, A.R. Hibbs, and D.F. Styer. *Quantum Mechanics and Path Integrals.* Dover books on physics. Dover Publications, Incorporated, 2010.

[16] S Florens, D Venturelli, and R Narayanan. Quantum phase transition in the spin boson model. In *Quantum Quenching, Annealing and Computation*, pages 145–162. Springer, 2010.

[17] Jay Gambetta and Howard Mark Wiseman. Non-markovian stochastic schrödinger equations: Generalization to real-valued noise using quantum-measurement theory. *Physical Review A*, 66(1):012108, 2002.

[18] Congjun Gan, Peihao Huang, and Hang Zheng. Non-markovian dynamics of a biased qubit coupled to a structured bath. *Journal of Physics: Condensed Matter*, 22(11):115301, 2010.

[19] Crispin Gardiner and Peter Zoller. *Quantum noise: a handbook of Markovian and non-Markovian quantum stochastic methods with applications to quantum optics*, volume 56. Springer, 2004.

[20] Crispin W Gardiner et al. *Handbook of stochastic methods*, volume 3. Springer Berlin, 1985.

[21] Jie Hu, Meng Luo, Feng Jiang, Rui-Xue Xu, and YiJing Yan. Padé spectrum decompositions of quantum distribution functions and optimal hierarchical equations of motion construction for quantum open systems. *The Journal of Chemical Physics*, 134(24):244106, 2011.

[22] Jie Hu, Rui-Xue Xu, and YiJing Yan. Communication: Padé spectrum decomposition of fermi function and bose function. *The Journal of chemical physics*, 133:101106, 2010.

[23] Peihao Huang and H Zheng. Quantum dynamics of a qubit coupled with a structured bath. *Journal of Physics: Condensed Matter*, 20(39):395233, 2008.

[24] Akihito Ishizaki and Graham R Fleming. Theoretical examination of quantum coherence in a photosynthetic system at physiological temperature. *Proceedings of the National Academy of Sciences*, 106(41):17255–17260, 2009.

[25] Edwin T Jaynes and Frederick W Cummings. Comparison of quantum and semiclassical radiation theories with application to the beam maser. *Proceedings of the IEEE*, 51(1):89–109, 1963.

[26] Jun Jing, Xinyu Zhao, J. Q. You, and Ting Yu. Time-local quantum-state-diffusion equation for multilevel quantum systems. *Phys. Rev. A*, 85:042106, Apr 2012.

[27] Sven Krönke and Walter T Strunz. Non-markovian quantum trajectories, instruments and time-continuous measurements. *Journal of Physics A: Mathematical and Theoretical*, 45(5):055305, 2012.

[28] A. J. Leggett, S. Chakravarty, A. T. Dorsey, Matthew P. A. Fisher, Anupam Garg, and W. Zwerger. Dynamics of the dissipative two-state system. *Rev. Mod. Phys.*, 59:1–85, Jan 1987.

[29] Goran Lindblad. On the generators of quantum dynamical semigroups. *Communications in Mathematical Physics*, 48(2):119–130, 1976.

[30] V. May and O. Kühn. *Charge and Energy Transfer Dynamics in Molecular Systems*. Wiley, 2011.

[31] Christoph Meier and David J Tannor. Non-markovian evolution of the density operator in the presence of strong laser fields. *The Journal of chemical physics*, 111:3365, 1999.

[32] T Niemczyk, F Deppe, H Huebl, EP Menzel, F Hocke, MJ Schwarz, Juan José García-Ripoll, David Zueco, T Hümmer, Enrique Solano, et al. Circuit quantum electrodynamics in the ultrastrong-coupling regime. *Nature Physics*, 6(10):772–776, 2010.

[33] EA Novikov. Functionals and the random-force method in turbulence theory. *Sov. Phys. JETP*, 20(5):1290–1294, 1965.

[34] Bernt Øksendal. *Stochastic differential equations*. Springer, 2003.

[35] Ian Percival. *Quantum state diffusion*. Cambridge University Press, 1998.

[36] Elizabeth L Read, Gabriela S Schlau-Cohen, Gregory S Engel, Jianzhong Wen, Robert E Blankenship, and Graham R Fleming. Visualization of excitonic structure in the fenna-matthews-olson photosynthetic complex by polarization-dependent two-dimensional electronic spectroscopy. *Biophysical journal*, 95(2):847–856, 2008.

[37] Gerhard Ritschel and Alexander Eisfeld. On analytic bath correlation functions obtained from broader class of spectral densities. *!!!To be annonounced!!!*

[38] Gerhard Ritschel, Jan Roden, Walter T Strunz, Alán Aspuru-Guzik, and Alexander Eisfeld. Absence of quantum oscillations and dependence on site energies in electronic excitation transfer in the fenna–matthews–olson trimer. *The Journal of Physical Chemistry Letters*, 2(22):2912–2917, 2011.

[39] Gerhard Ritschel, Jan Roden, Walter T Strunz, and Alexander Eisfeld. An efficient method to calculate excitation energy transfer in light-harvesting systems: application to the fenna–matthews–olson complex. *New Journal of Physics*, 13(11):113034, 2011.

[40] Jan Roden, Alexander Eisfeld, Matthieu Dvořák, Oliver Bünermann, and Frank Stienkemeier. Vibronic line shapes of ptcda oligomers in helium nanodroplets. *The Journal of chemical physics*, 134:054907, 2011.

[41] Jan Roden, Alexander Eisfeld, Wolfgang Wolff, and Walter T. Strunz. Influence of complex exciton-phonon coupling on optical absorption and energy transfer of quantum aggregates. *Physical Review Letters*, 103(5):058301, 2009.

[42] Jan Roden, Walter T. Strunz, and Alexander Eisfeld. Non-markovian quantum state diffusion for absorption spectra of molecular aggregates. *The Journal of Chemical Physics*, 134(3):034902, 2011.

[43] Wolfgang P Schleich. *Quantum optics in phase space*. Wiley. com, 2011.

[44] Marcel Schmidt am Busch, Frank Mu h, Mohamed El-Amine Madjet, and Thomas Renger. The eighth bacteriochlorophyll completes the excitation energy funnel in the fmo protein. *The Journal of Physical Chemistry Letters*, 2(2):93–98, 2010.

[45] Schrödinger, LLC. The PyMOL molecular graphics system, version 1.3r1. August 2010.

[46] Walter T. Strunz. Linear quantum state diffusion for non-markovian open quantum systems. *Physics Letters A*, 224(1–2):25 – 30, 1996.

[47] Walter T. Strunz. Stochastic schrödinger equation approach to the dynamics of non-Markovian open quantum systems. Habilitation thesis, June 2001.

[48] Walter T. Strunz, Lajos Diósi, and Nicolas Gisin. Open system dynamics with non-markovian quantum trajectories. *Phys. Rev. Lett.*, 82:1801–1805, Mar 1999.

[49] Johan Strümpfer and Klaus Schulten. Open quantum dynamics calculations with the hierarchy equations of motion on parallel computers. *Journal of chemical theory and computation*, 8(8):2808–2816, 2012.

[50] D. Tronrud, A. Camara-Artigas, R. Blankenship, and J.P. Allen. Crystal structure of the fenna-matthews-olson protein from chlorobaculum tepidum, May 2009.

[51] Daniel F Walls and G Gerard J Milburn. *Quantum optics*. Springer, 2008.

[52] U. Weiss. *Quantum Dissipative Systems (Second Edition)*. Series in Modern Condensed Matter Physics. World Scientific Publishing Company Incorporated, 1999.

[53] Howard M Wiseman and Gerard J Milburn. *Quantum measurement and control.* Cambridge University Press, 2010.

[54] Ting Yu. Non-markovian quantum trajectories versus master equations: Finite-temperature heat bath. *Physical Review A*, 69(6):062107, 2004.

[55] Ting Yu, Lajos Diósi, Nicolas Gisin, and Walter T. Strunz. Non-markovian quantum-state diffusion: Perturbation approach. *Phys. Rev. A*, 60:91–103, Jul 1999.

[56] Ting Yu, Lajos Diosi, Nicolas Gisin, and Walter T Strunz. Post-markov master equation for the dynamics of open quantum systems. *Physics Letters A*, 265(5):331–336, 2000.